European Train the Trainer Programme for Responders

Lecture 5

Safety of liquid hydrogen

LEVEL IV

Specialist officer

The information contained in this lecture is targeted at the level of specialist officer and above.

This topic is also available at levels I and III

This lecture is part of a training material package with materials at levels I – IV : Firefighter, crew commander, incident commander and specialist officer. Please see the lecture introduction regarding competence and learning expectations

Note: these materials are the property of the HyResponder Consortium and should be acknowledged accordingly, the outputs of PRESLHY have been used as a basis

Co-funded by the European Union

Disclaimer

Acknowledgments

This project has received funding from the Fuel Cells and Hydrogen 2 Joint Undertaking (now Clean Hydrogen Partnership) under Grant Agreement No 875089. This Joint Undertaking receives support from the European Union's Horizon 2020 Research and Innovation program, Hydrogen Europe and Hydrogen Europe Research. The Deliverable 6.1 – Handbook of hydrogen safety: Chapter on LH2 safety – of Pre-normative REsearch for Safe use of Liquid Hydrogen (PRESLHY) project (grant agreement number 779613) is also acknowledged.

Summary

For various applications of hydrogen where volume is an essential issue, liquid hydrogen (LH_2) is a necessary for the sake of volume reduction. However, there are also other situations where the liquid state represents a reasonable and economic solution for storage and distribution of large amounts of hydrogen depending on the end-user's requirements. Furthermore, LH_2 has the advantage of extreme cleanliness making it appropriate in many industrial applications. Major drawback is the enormous energy input required to liquefy the hydrogen gas, which has a significant impact on the economy of handling LH_2.

The hazards associated with the presence and operation of LH_2 containing systems are subject of safety and risk assessments. Essential part of such accident sequence analyses is the simulation of the physical phenomena which occur in connection with the inadvertent release of LH_2 into the environment by computation models. The behaviour of cryogenic pool propagation and vaporization on either a liquid or a solid ground as well as potential pool burning is principally well understood. Furthermore, state-of-the-art computer models have been developed and validated against respective experimental data. There are, however, still open questions which require further efforts to extent the still poor experimental data basis.

This lecture is based on the Deliverable 6.1 – Handbook of hydrogen safety: Chapter on LH2 safety – of Pre-normative REsearch for Safe use of Liquid Hydrogen (PRESLHY) project. The experimental and theoretical investigation of the characteristics of liquid hydrogen, its favourable and unfavourable properties, as well as the lessons learnt from accidents have led to a set of codes, standards, regulations, and guidelines, which resulted in a high level of safety achieved today. This applies to both LH_2 production and the methods of mobile or stationary LH_2 storage and transportation/distribution, and its application in both science and industries.

Keywords

Liquid hydrogen, cryogenic release, accidental spill, combustion, liquid hydrogen technology

Table of contents

Summary 3

Keywords 3

1. Target audience 6
  - 1.1 Roll description: Specialist 6
  - 1.2 Competence level: Specialist 6
  - 1.3 Prior learning: Specialist 6

2. Introduction and objectives 6

3. Liquid hydrogen properties 7
  - 3.1 Physical properties 7
  - 3.2 Chemical properties 11

4. Liquid hydrogen hazards 13
  - 4.1 Impact of cryogenic hydrogen on materials 14
  - 4.2 Physiological problems with cryogenic hydrogen 16
  - 4.3 Immediate ignition of pressurised LH_2 release 17
  - 4.4 Delayed ignition of pressurised LH_2 release 17
  - 4.5 Cryogenic hydrogen pool vaporisation 18
  - 4.6 Unconfined vapour cloud explosion (UVCE) 18
  - 4.7 BLEVE phenomenon 18
  - 4.8 RPT phenomenon 20
  - 4.9 Purely cryogenic hazards 21

5. Cryogenic release 22
  - 5.1 Single-Phase Releases 22
  - 5.2 Multi-Phase Releases 23

6. Combustion 24
  - 6.1 Cryogenic jet fires 24
    - 6.1.1 Thermal loads 24
    - 6.1.2 Pressure loads from delayed ignition 25
    - 6.1.3 Pressure peaking phenomenon 25
  - 6.2 Liquid pool burning 26
    - 6.2.1 Phenomenology 26
    - 6.2.2 Experimental work 27
  - 6.3 Deflagration of cold hydrogen-air mixture 31

7. Liquid hydrogen technology 34

7.1 Liquid hydrogen production process and infrastructures 34
7.2 Liquid hydrogen storage and transport 36
  7.2.1 Liquid hydrogen storage 36
  7.2.2 Cryostat for stationary applications 40
  7.2.3 Cryostat for mobile applications 41
  7.2.4 Liquid hydrogen transport 42
7.3 Liquid hydrogen refuelling station 50
7.4 Liquid hydrogen systems for mobility 54
  7.4.1 Cars 54
  7.4.2 Buses 56
  7.4.3 Trucks 57
  7.4.4 Ships 58
  7.4.5 Aircrafts 60
8. Liquid hydrogen hazards and associated risk for Responders 62
9. Safety measures and engineering solutions 64
References 65

1. Target audience

The information contained in this lecture is targeted at the level of specialist officer and above. This lecture is also available at levels I: Fire fighter.

The role description, competence level and learning expectations assumed at specialist officer level are described below.

1.1 Roll description: Specialist

Specialists assist Incident Commanders with advice and by directing and supervising technical operations that involve the use of knowledge, skills or equipment related to a specific risk or response activity. Typical incidents involve hazardous materials, transportation vehicles, climatic events, structural and other built environment failures and emergency response logistics.

1.2 Competence level: Specialist

A scientific, engineering and empirical foundation in the subject area with skills, extended by experience, to apply that information, knowledge in an interpreted and useful way to enable the Incident Commander and other first responders under the specialist's direction to respond effectively and safety to the emergency situation.

1.3 Prior learning: Specialist

EQF 5 Comprehensive, specialised, factual and theoretical knowledge within a field of work or study and an awareness of the boundaries of that knowledge. A comprehensive range of cognitive and practical skills required to develop creative solutions to abstract problems. Exercise management and supervision in contexts of work or study activities where there is unpredictable change; review and develop performance of self and others.

2. Introduction and objectives

The use of liquid hydrogen (LH_2) in practical applications is of great interest due to the higher energy density of LH_2 in comparison with that of compressed gaseous hydrogen (cGH_2). LH_2 is typically used as a concentrated form of hydrogen storage. As for any gas, storing it as liquid takes less space than storing it as a gas. The density of LH_2 is only 70.8 kg m^{-3} at standard pressure and boiling temperature (1 atm, 20.3 K). LH_2 requires cryogenic storage technology such as special thermally insulated containers and requires special handling common to all cryogenic fuels, which bring potential risks for LH_2 generation, transportation and application.

The aim of this lecture is to provide responders with sufficient knowledge and the potential hazards of LH_2, helping responders to understand the properties and behaviour of LH_2.

By the end of this lecture responders will be able to:

- Understand the properties, in terms of physical and chemical, of LH_2;

- Know the hazards of cryogenic hydrogen;
- Recognise the release and combustion of cryogenic hydrogen and the thermal and pressure hazards;
- Be familiar with the technologies of LH_2 generation, storage, and transport.
- Identify the risk and hazard of LH_2 pertinent to responders.

3. Liquid hydrogen properties

3.1 Physical properties

Liquid hydrogen (LH_2) is the liquid state of the element hydrogen. To exist as a liquid, hydrogen must be cooled below its critical point of 33 K. However, for it to be in a fully liquid state at atmospheric pressure, hydrogen needs to be cooled to 20.28 K (−252.87 °C) [1]. The triple point of hydrogen is at 13.81 K [1] and 7.042 kPa [2]. Liquid hydrogen also has a much higher specific energy than gasoline, natural gas, or diesel. Liquid hydrogen is typically used as a concentrated form of hydrogen storage. As for any gas, storing it as liquid takes less space than storing it as a gas at normal temperature and pressure. However, the liquid density is very low compared to other common fuels. Once liquefied, it can be maintained as a liquid in pressurized and thermally insulated containers. The density of liquid hydrogen is only 70.99 g/L (at 20 K), a relative density of just 0.07 (Figure 1). The energy density of hydrogen is very high; 1 kg of hydrogen contains approximately 2.5 times more energy than 1 kg of natural gas. Although the specific energy is more than twice that of other fuels, this gives it a remarkably low volumetric energy density, many folds lower. The main properties of LH_2 are summarised in Table 1.

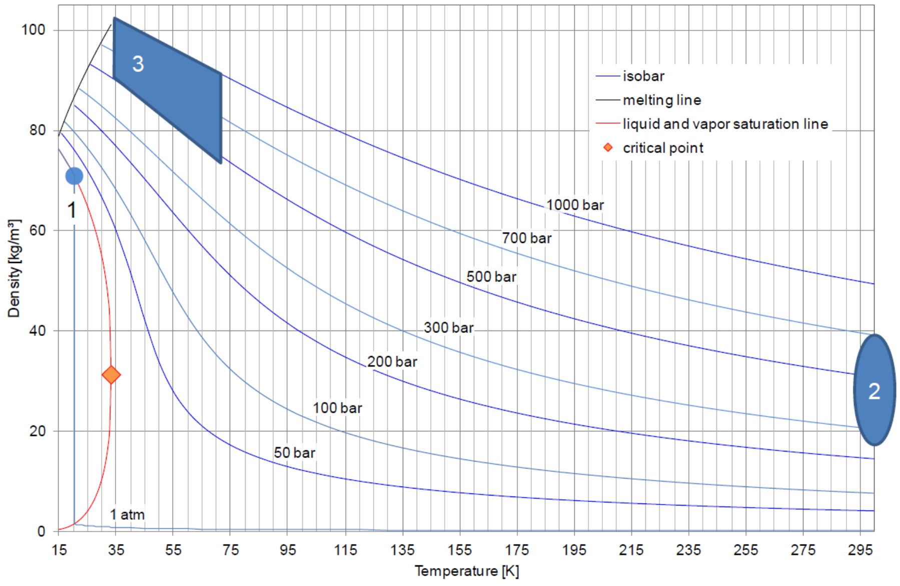

1 - liquid @ ~20 K; 2 - pressurised gas @ ~300 K; 3 - cryogenic compressed gas

Figure 1. Density of hydrogen in the low temperature range as a function of pressure [3].

When handling LH_2 in confined areas, a hazard is given by the fact that due to the volume increase by a factor of 845, when LH_2 is heated up from its boiling point (20.369 K) to ambient conditions, the composition of the local atmosphere may change drastically. In an enclosed space completely filled with LH_2, final pressure after warm-up to 300 K may rise to a theoretical estimate of 172 MPa which certainly overpressurizes systems to bursting [4].

A further temperature decrease below the boiling point eventually results in the generation of solid hydrogen. Mixtures of coexisting liquid and solid hydrogen or slush hydrogen (SLH_2) offer the advantages of a higher density by up to 16%, a higher heat capacity by up to 18%, and a prolongation of the storage time of the cryogen as the solid melts and absorbs heat. Therefore, it is of particular interest to use slush as a rocket fuel in space missions. Due to the fact that the hydrogen vapor pressure is strongly reduced with decreasing temperatures, from 98 kPa (which is about atmospheric pressure) at 20 K down to 13 kPa at 13 K, SLH_2 systems must be designed to safely operate below atmospheric pressure. At a pressure below ambient pressure the storage system must be protected against air ingress, which represents a hazard.

At the triple point of hydrogen with the temperature of 13.8 K and a pressure of 7.2 kPa, all three phases can exist in equilibrium (Figure 2). The boiling point increases with pressure to the critical point which is given by T_c = 33.15 K, p_c = 1.296 MPa with a critical density of γ_c = 31.4 kg/m³. A pressure increase beyond the critical point has no further influence.

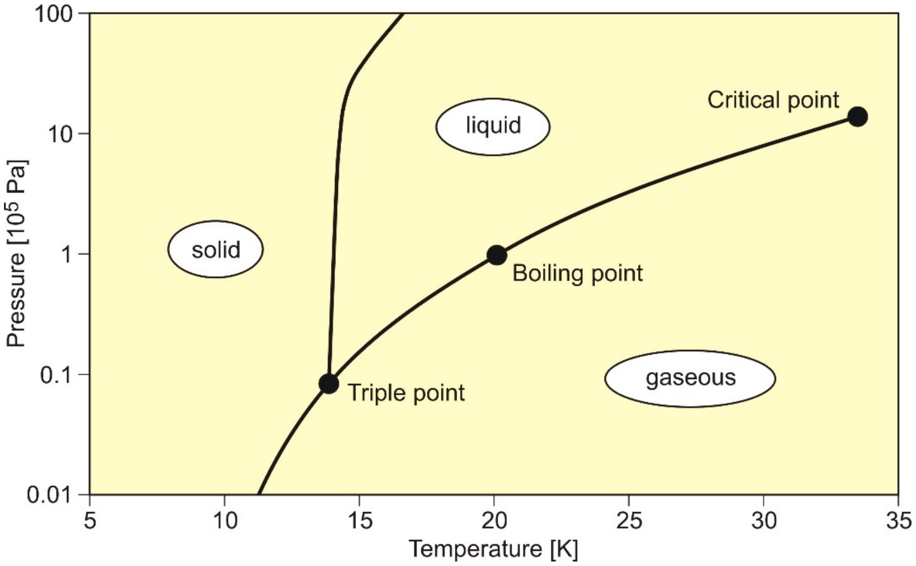

Figure 2. Phase diagram of hydrogen.

There is no liquid phase of hydrogen existing above its critical temperature. If a fluid is heated and maintained above its critical temperature, it becomes impossible to liquefy it with pressure. When pressure is applied, a single phase "supercritical fluid" forms which is characterized by T_c and p_c. "Supercritical" generally refers to conditions above the critical temperature and close to the critical pressure. It has characteristics similar to a gas and a liquid without changing its chemical structure. It is gas-like in that it is compressible and easily diffuses through materials;

it is liquid-like in that it has a comparable density and may dissolve materials. And there are some transition states in between characterized by strong structural fluctuations causing the unusual behaviour of fluids near the critical point covering all scales from microscopic to macroscopic.

Due to the strong dependence on temperature and pressure in the supercritical state, the thermophysical properties of cryogenic hydrogen vary strongly especially in the near-critical region. By proper control of pressure and temperature, one can access a significant range of physico-chemical properties, i.e. density, viscosity, diffusivity, without passing through a phase boundary. The specific heat capacity has a maximum at the so-called pseudo-critical temperature. Also, the isothermal compressibility is particularly large just above the critical temperature; at the critical point, it tends to infinity. For a highly compressible fluid, a small temperature gradient implies a large density gradient. It exhibits higher flow rates as compared with liquids. An important factor may be that the fluid might undergo a turbulent-to-laminar transition due to the dependence of viscosity on temperature. Heat transfer coefficients are unpredictable in the transition regime and are much lower in the laminar regime.

Hydrogen coexists in two isomeric forms, ortho and para hydrogen. A small energetic difference is given, if the spins of the two protons of a hydrogen molecule are either aligned parallel (ortho) or anti-parallel (para). The existence of the two forms was proven experimentally in 1929 by Bonhoeffer and Harteck [5] using charcoal as catalyst for the separation. The partition is dependent on the temperature (Figure 3). Normal hydrogen at room temperature is a mixture of 75% ortho and 25% para hydrogen. In the lower temperature range < 80 K, para hydrogen is the more stable form. At 20 K, in thermal equilibrium, the concentrations are 99.825% para and 0.175% ortho. The rate of conversion between ortho and para states is with 0.0114 h^{-1} slow in the gas phase. The non-catalysed transition takes place over a longer period (about 3–4 days), until a new equilibrium state is reached. However, magnetic materials and small oxygen concentrations can accelerate ortho-para conversion raising the rate by several orders of magnitude to the order of hours. $Fe(OH)_3$ is used in many technical applications as a very good catalyst for the conversion.

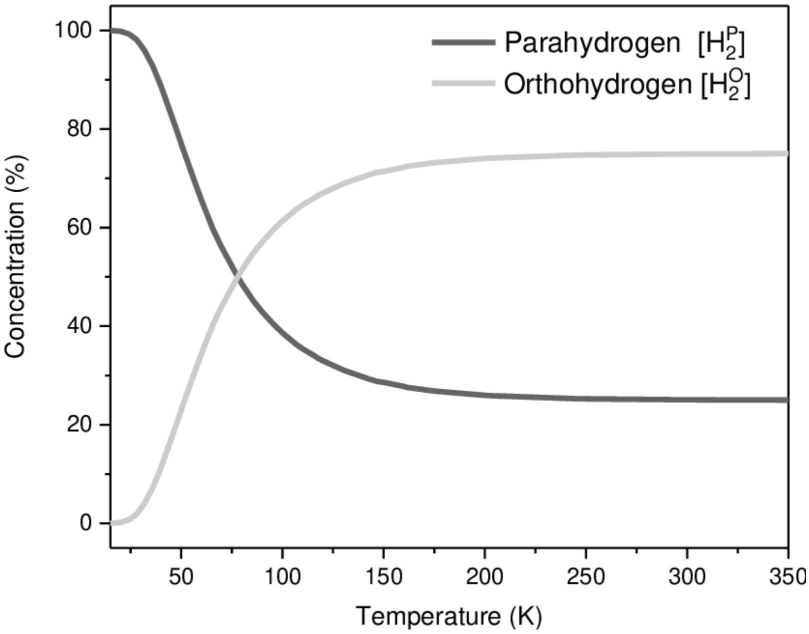

Figure 3. Equilibrium concentration of ortho- and para-hydrogen vs. temperature [6].

The conversion from ortho to para is an exothermal reaction with a conversion energy of 270 kJ/kg at room temperature which increases with decreasing temperature. At temperatures below 77 K, it is almost constant at 523 kJ/kg. The liberated heat of ortho-para conversion is larger than the latent heat of vaporization/condensation (446 kJ/kg at the same temperature), which means that normal liquid hydrogen is able to vaporize completely even in a perfectly insulated vessel. It therefore represents a safety issue requiring a design of the LH_2 containing systems to be able to remove the heat of ortho-para conversion in a safe manner.

For internal cooling of gases adiabatic ideal throttling process may be applied. This so-called Joule-Thomson effect arises from the forces between the gas molecules. It is “internal work” against or in the direction of the van der Waals forces acting among the molecules. This means that the temperature of a real gas decreases below the inversion temperature ($T < T_I$) or increases above this temperature ($T > T_I$) upon expansion (depressurization) at constant enthalpy.

The Joule-Thomson effect is quantified with the Joule-Thomson coefficient, describing the temperature change by changing pressure at constant enthalpy:

$$\mu_{TJ} = \left(\frac{dT}{dp}\right)_H \tag{1}$$

It is negative if the temperature is decreasing, and positive for an increasing temperature. It is zero for an ideal gas or at the inversion temperature. Thus, all locations where there is no temperature change are forming the so-called inversion curve shown for hydrogen as a real gas, see Figure 4. Unlike most other gases, the inversion temperature of H_2 gas is 193 K at atmospheric pressure, much lower than ambient temperature. A safety concern is that the sudden depressurization of a GH_2 storage vessel may lead to an ignition because of the negative

Joule-Thomson coefficient of hydrogen at standard temperature. The actual temperature increase, however, is only 6 K, if a sudden pressure drop from 20 MPa to ambient pressure takes place. The chance of a spontaneous ignition just by that effect is small. Ignition is more likely to occur because of electrostatic charging of dust particles during the depressurization or auto-ignition, shock diffusion ignition, or other mechanisms such as spark discharges from isolated conductors, brush discharges, corona discharges [7].

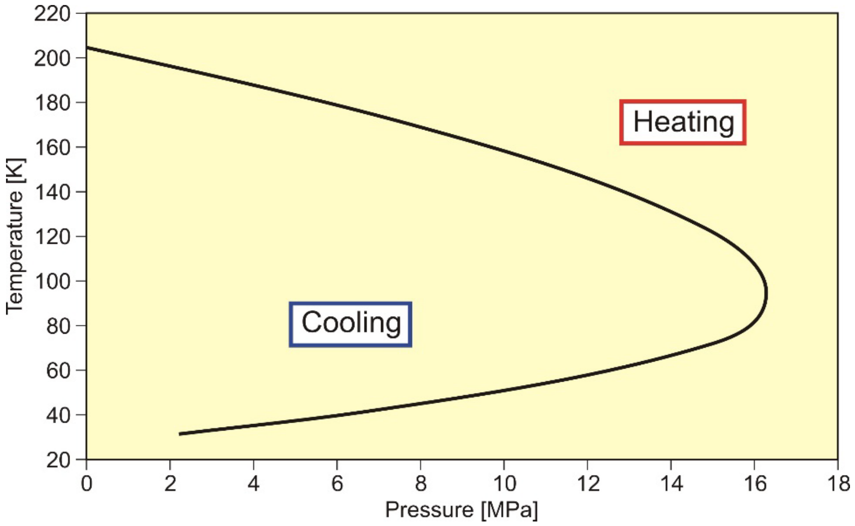

Figure 4. Inversion temperature of hydrogen.

3.2 Chemical properties

Hydrogen is able to react chemically with most other elements. In connection with oxygen, hydrogen is highly flammable over a wide range of concentrations. It burns in a non-luminous hot flame to water vapor liberating the chemically bound energy as heat (gross heat of combustion: 286 kJ/mol). A stoichiometric hydrogen-air mixture contains 29.5 vol% of hydrogen. The flammability range is of 4–75 vol% of concentration in air, up to 95 vol% in oxygen, and widens with increasing temperatures. The lower flammability limit (LFL) as the minimum amount of fuel that supports combustion, is usually the more important limit for low-rate releases, since it will be reached first in a continuous leakage. Most importantly, the cloud with > 4% hydrogen concentration may cover longer distances and larger area from the releases point. The influence of the temperature is expressed in the modified Burgess-Wheeler equation for the LFL, which is for hydrogen (at ambient pressure) [8]:

$$c_{LFL} = c_{LFL}(300\,K) - \frac{3.14}{\Delta H_c}(T - 300) = 4.0 - 0.013\left(T - 300\right)\ \left(vol\%\right) \qquad (2)$$

where ΔH_c – net heat of combustion, = 242 kJ/mol; T – temperature, K.

For just vaporized hydrogen at the boiling point, the LFL is 7.7%. The respective equation for the upper flammability limit (UFL) is [9]:

$$c_{UFL} = 74.0 + 0.026\left(T - 300\right)\ \left(vol\%\right) \qquad (3)$$

valid for the temperature range $150 \leq T \leq 300$, with T in K.

A more recent experimental study [10] concludes a slightly modified linear relationship between flammability limits and temperature recommending the following equations:

$$c_{LFL} = 4.64 - 0.0067\,T \quad (vol\%) \tag{4}$$

in the temperature range -150°C ≤ T ≤ 400°C, and

$$c_{UFL} = 73.8 + 0.033\,T \quad (vol\%) \tag{5}$$

in the temperature range -60°C ≤ T ≤ 400°C.

All above LFL and UFL correlations are depicted in Figure 5.

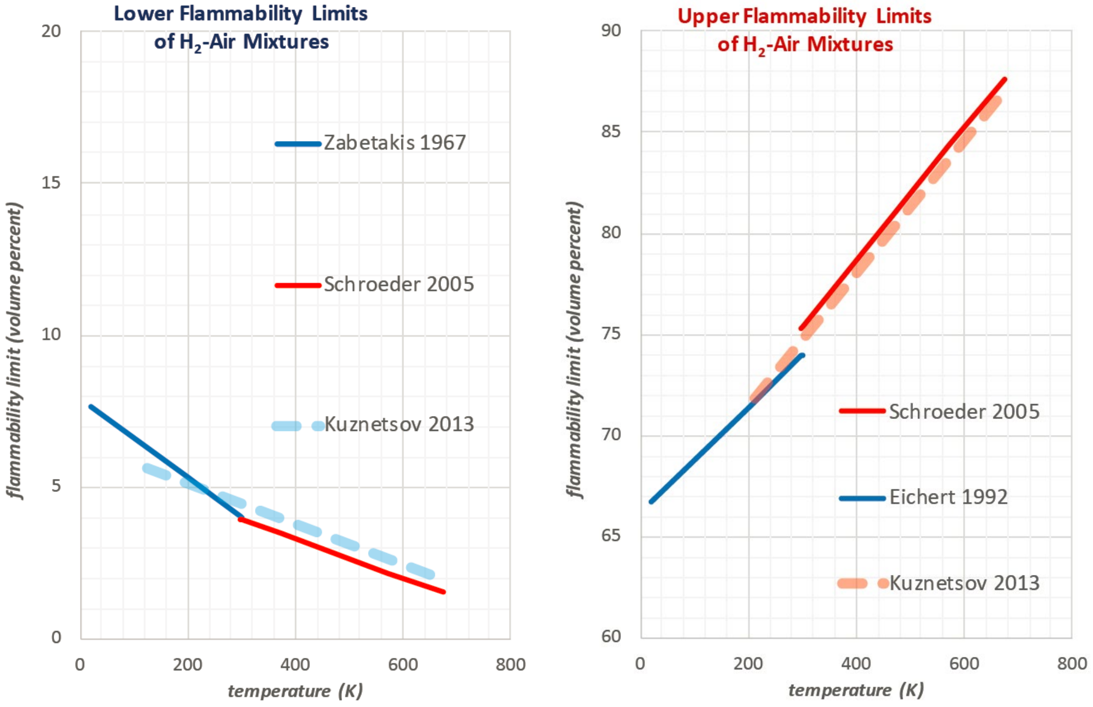

Figure 5. Flammability limits in hydrogen-air mixtures, LFL (left) and UFL (right) [8-10].

The auto-ignition temperature of 858 K is relatively high but can be lowered by catalytic surfaces. The minimum ignition energy at stoichiometric mixture is 17 µJ (ambient temperature, pressure and ignition of hydrogen in normal air composition), much lower than for hydrocarbon-air mixtures. A weak spark or the electrostatic discharge by a human body, which is in the range of 10 mJ, would suffice for an ignition; this is, however, no different from other burnable gases. The minimum ignition energy is even further decreasing with increasing temperature, pressure, or oxygen contents. Measurements at cryogenic temperatures have been provided recently [11].

For open LH_2 pools, it needs to be considered that cold hydrogen gas is less volatile compared to ambient gas and thus more prone to the formation of a flammable mixture with air. Furthermore, LH_2 in direct contact with the ambient air quickly contaminates itself due to condensation and solidification of air constituents. Solid particles may lead to plugging of pressure relief valves, vents or filters. In addition, due to the different boiling points of nitrogen (77.3 K) and oxygen (90.2 K), the oxygen condenses first upon cooling down or vaporizes last upon warming up, both situations always connected with an oxygen-enriched condensate forming shock-explosive mixtures. In addition, liquid or solid oxygen in combination with another combustible material, even if solid and thus not "flammable", may form highly explosive mixtures with drastically decreased ignition energies. Examples are LH_2 plus solid air having an O_2 fraction of > 40%, or liquid oxygen spilled onto asphalt [8].

4. Liquid hydrogen hazards

Liquid hydrogen requires cryogenic storage technology such as special thermally insulated containers and requires special handling common to all cryogenic fuels. This is similar to, but more severe than liquid oxygen. Even with thermally insulated containers it is difficult to keep such a low temperature, and the hydrogen will gradually leak away. It also shares many of the same safety issues as other forms of hydrogen, as well as being cold enough to liquefy, or even solidify atmospheric oxygen, which can be an explosion hazard.

Due to liquid hydrogen characteristics and requirements of hydrogen energy applications, LH_2 used in confined configuration are out of the scope of HyResponder project. A review of the existing literature on physical phenomena associated with LH_2 was performed in the PRESLHY project (D2.2 "State of the art analysis", 2018). On this basis, in order to define the different hazardous scenarios and associated consequences, LH_2 storage is considered only. Table 1 summarizes these events, with initial causes and potential final consequences.

Table 1. Description of potential hazardous events.

Feared events	Main conditions	Consequences
1 - Burst of the storage at working pressure (P_W) (impinging fire / fragment)	100% gaseous H_2 - 10 bar - type I vessel	Overpressure and fragments
2 - Accidental event on storage with liquid H_2 (fire case) at $2P_W$	Burst of LH_2 storage Flash fire	“BLEVE” with thermal effects
3 - Failure on the storage (breech or perforation)	10 bar, rapid liquid H_2 spreading and evaporation on ground	Pool vaporization and cryogenic cloud formation with overpressure effects in case of flammable cloud ignition
4 - Leak on the pipe between storage and pump	10 bar, liquid * diphasic pressurized release * and/or H_2 liquid pool, vaporization forming a flammable cloud	Liquid hydrogen jet and potential rainout forming a LH_2 pool on the ground and overpressure effects due to flammable mixture ignition
5 - Leak on the pipe between pump and atm. vaporizer	1000 bar, liquid * diphasic pressurized release but behaving like a high pressure gaseous jet	Certainly nearly-gaseous high pressure jet behaviour with overpressure effects due to ignition
6 - Burst of the storage at rupture pressure (P_R)	100% gaseous - 10 bar, type I	Overpressure and fragments

Note: BLEVE – boiling liquid expanding vapour explosion.

Regarding scenarios previously summarized, it can be highlighted that some of them are specific of liquid hydrogen, and other are gaseous feared events are already described, or similar.

Behaviour of liquid hydrogen release, and thus associated consequences, will depend on the initial pressure. That is the reason why in the Table 1 for each feared event, details are given on the pressure and on the state of hydrogen.

4.1 Impact of cryogenic hydrogen on materials

The stress which a structural material is able to withstand is determined by its ductility (Figure 6). A material is elastic if, after being elongated under stress, it returns to its original shape and volume as soon as the stress is removed. At a certain strain, it departs from linearity, i.e. the material will retain a permanent elongation which is attributed to plastic deformation behaviour. The applied stress is the so-called “yield stress”. With a further increase of the strain eventually the “ultimate or tensile stress” is reached, beyond which the stress steadily decreases until rupture. In contrast, a brittle material does not exhibit a permanent plastic elongation phase and rather breaks abruptly without any warning as soon as it is exposed to its tensile stress [5].

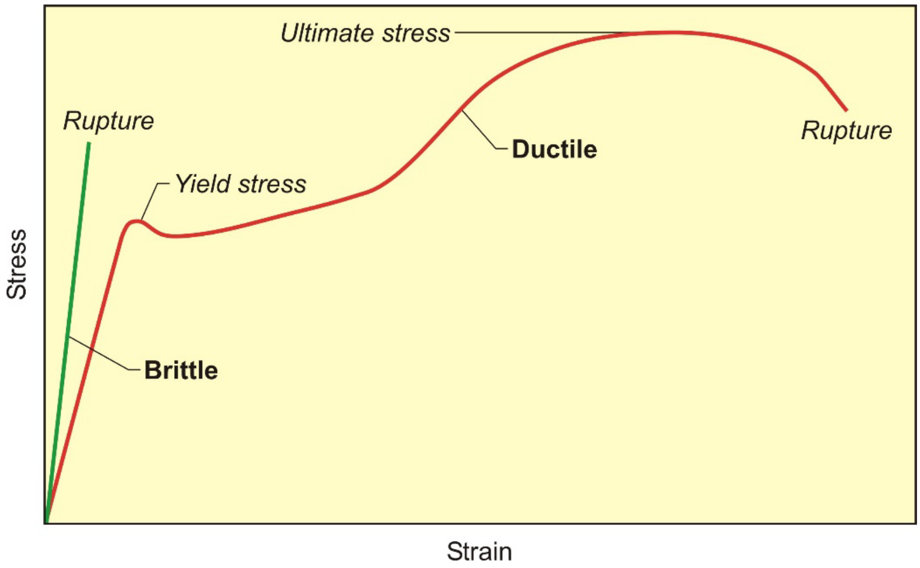

Figure 6. Ductile and brittle behaviour of materials [5].

Hydrogen has long been recognized to have a deleterious effect on some metals by changing their physical properties. It is basically due to the presence of hydrogen atoms dissolved in the metal grid and accumulating in disturbed lattice regions. Apart from this hydrogen embrittlement effect, there is an additional influence on structural materials at cryogenic temperatures, which accounts for most service failures of brittle-type materials. With decreasing temperature, the yield stress and ultimate stress increase for most metals, generally connected with a corresponding drop in fracture toughness which is a measure of the ability of materials to resist crack propagation. The lower the toughness, the smaller is the tolerable crack length.

A material can change from ductile to brittle behaviour as soon as the temperature falls below its so-called “nil-ductility temperature”. This temperature is not a fixed value but may vary as a function of prior heat or mechanical treatment and of the alloy composition and impurities, respectively. It is, in principle, the minimum temperature, at which a structural material is considered useful and can sometimes be significantly higher than the temperature of the cryogen. For some materials at cryogenic temperature, little stress is sufficient to break it, and it can occur very rapidly resulting in an almost instantaneous failure. This effect is a particular problem in cryogenic equipment exposed to periodic changes and was found in several accidents to have caused the failure of a cryogenic storage vessel, e.g. the rupture of a 4250 m^3 LNG tank in Cleveland, USA, in 1944 [8], when material behaviour at cryogenic temperatures was not yet deeply understood.

The components of a cryogenic system usually undergo a thermal gradient, some only during cool-down or warm-up phases, others even at steady state operation. Strong gradients, particularly if non-linear, result in stresses which may lead to rupture. Thermal gradients are of significance in systems with stratified two-phase flows of cryogens.

Low temperatures can also affect materials by thermal contraction causing large thermal stresses, if the system cannot accommodate the differential thermal contraction of the materials. The thermal expansion coefficient is a function of the temperature. For many materials which are cooled down to cryogenic temperatures, more than 90% of the total contraction will have already taken place until 77 K. The coefficient is approximately 0.3% in iron-based alloys, 0.4% in aluminium, or more than 1% in many plastics [5, 12]. Cryogenic vessels or piping must account for this contraction to avoid large thermal stresses.

Materials with sufficiently high strength and high ductility, working successfully at low temperatures, including aluminium and most of its alloys, copper and its alloys, nickel and some of its alloys, as well as austenitic stainless steels, should be used in cryogen containing systems.

For many materials, specific heat exhibits a strong temperature dependence below 200 K showing that at cryogenic temperatures, much less heat is required to raise the temperature of a body than at ambient temperatures. An example: heat capacity of aluminium is reduced from about 950 J/(kg·K) at ambient temperature to less than 10 J/(kg·K) at 20 K.

4.2 Physiological problems with cryogenic hydrogen

Hydrogen is classified as non-toxic and non-acid, non-carcinogenous, being a simple asphyxiant with no threshold limit value (TLV) or LD50 (lethal dose 50%) value established [12].

Vaporization of released liquid hydrogen affects the composition of the atmosphere, particularly in (partially) confined areas, carrying the risk of asphyxiation. The enormous liquid/ambient expansion ratio combined with condensation of O_2 from the ambient air and burning of flammable H_2-air mixtures leads to a significant dilution of the local atmosphere. An oxygen volume fraction of less than 19.5% is considered by NASA to be dangerous to humans; less than 8% will be lethal within minutes (Table 2). Alarm levels are generally set at 19% of oxygen.

Table 2. Impact on humans by an atmosphere with decreasing oxygen contents.

Oxygen contents in air (%)	Symptoms
~21 – 19	None
~19 – 15	Reduced reaction times, no visible effects
~15 – 12	Heavy breathing, rapid heart beat, impaired attention or coordination
~12 – 10	Dizziness, faulty judgement, poor muscular coordination, rapid fatigue, lips slightly bluish
~10 – 8	Nausea, vomiting, inability to move, loss of consciousness followed by death
~8 – 6	Brain damage after 4–8 min, death within 8 min

< 6	Coma after 40 s, respiratory failure, death

Direct contact with liquid hydrogen or with surfaces at very low temperature causes cryogenic “burns” similar to thermal burns. Living tissue will freeze except for very brief contact periods where the temperature difference between cryogen and skin is still high (film boiling regime) and heat transfer small. The freezing of skin onto a cold surface can lead to severe damage upon removal. Prolonged skin exposure to cold hydrogen may result in frostbite. A symptom is short-lived local pain. Frozen tissues are painless and appear waxy, with a pale whitish or yellowish color. Thawing of the frozen tissue can cause intense pain. Shock may also occur. Prolonged inhalation of cold vapor or gas may cause serious lung damage. Particularly eyes are sensitive to cold. A longer exposure to cold temperatures after a large spill lowers the body temperature resulting in hypothermia, organ dysfunction, and respiratory depression [5].

There are no significant environmental hazards associated with the accidental discharge of liquid hydrogen due to its non-toxic character.

4.3 Immediate ignition of pressurised LH_2 release

Immediate ignition of a LH_2 high pressure jet seems to be similar to a gaseous hydrogen high pressure jet, with overpressure effects due to ignition. The work has shown that the similarity law can be applied for cryogenic unignited releases, and jet flame correlations developed for gaseous releases are also applicable [13].

4.4 Delayed ignition of pressurised LH_2 release

The higher density of the saturated hydrogen vapour at low temperatures may cause the hydrogen cloud to flow horizontally or downwards after immediate release of liquid hydrogen (should be accounted for during intervention at an accident scene). Usually, the condensation of atmospheric humidity will also add water to the mixture cloud (making it visible), making it even denser.

Figure 7. LH_2 large-scale release and delayed ignition (5 bar - 12 mm; PRESLHY project - HSE).

Due to liquid high density and vaporization at ambient temperature, the flammable cloud is significantly larger than the cloud induced by a gaseous hydrogen release (Figure 7). Therefore, consequences in case of ignition of this flammable cloud maybe more important in terms of intensity and distance of effects. If the pressure is low enough or release diameter large enough, in some conditions additionally to the hydrogen jet, a rain-out phenomenon (formation of hydrogen droplets falling on the ground and inducing a hydrogen pool) could be observed. In these cases, it is difficult to know which phenomenon - between jet or pool - will induce the most important consequence in case of ignition, or what will be the consequence of the combination of these two physical phenomena.

4.5 Cryogenic hydrogen pool vaporisation

A hydrogen liquid spillage can induce a pool. Liquid hydrogen will vaporize and form a flammable cloud with a significant volume. Wind conditions have a significant impact on the propagation and the dispersion of the cloud. Small-scale pool experiments were performed by KIT in 2020, showing no spontaneous ignition of hydrogen liquid pool. However, forced ignition (spark) above the pool highlighted the importance of the ground characteristics on the deflagration effects. Sand and concrete induce the same behaviour, but gravels escalated consequences.

Additionally, first simulations with the presence of a retention pit – aiming at limiting the spreading of the liquid – show a significant impact of this configuration on vaporization rate. In presence of retention pit, the vaporization rate of LH_2 would be significantly reduced, resulting in a smaller and long-lasting dispersed cloud. The dispersed cloud from a release scenario without retention pit would tend to propagate higher from the ground and die out quickly. Results must be confirmed with additional calculations and comparisons with other future experiments.

4.6 Unconfined vapour cloud explosion (UVCE)

In case of LH_2 spillage on an industrial site, a cold and reactive H_2/air cloud could be formed. In case of ignition, the flame could interact with the obstacles (vaporizer, pipe rack, vegetation) possibly leading to flame acceleration and even to a deflagration to detonation transition in the worst-case scenario.

4.7 BLEVE phenomenon

A BLEVE (boiling liquid expanding vapor explosion) is an event associated with the catastrophic failure of a pressure vessel containing a liquid which is stored at a temperature above its saturation temperature at atmospheric pressure. On failure, some of the liquid will flash to vapour resulting in the generation of overpressure, ignition of the released contents produces a large fireball which can determine the hazard range. This hazard is thus relevant to LH_2 which, although stored cryogenically, is also at modest pressure. Although LH_2 vessels are designed to relieve safely in the event of loss of the insulating vacuum, failure/blockage of this system could lead to a BLEVE, or fire attack could raise pressures and lead to a BLEVE with a fireball due to inadequate venting of pressure.

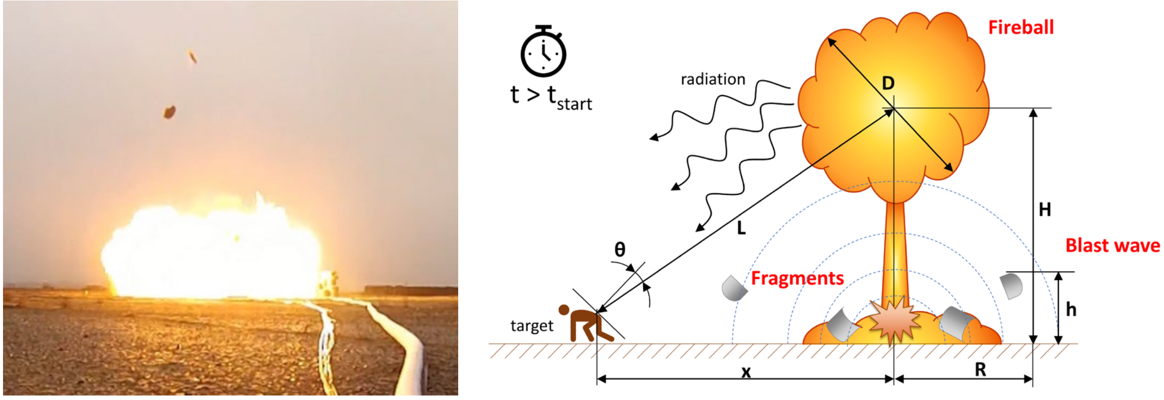

Figure 8. BLEVE main consequences (Photo: BLEVE on LNG tank) [17].

Many experimental and analytical studies on BLEVEs are available for substances, such as butane, propane, LNG, etc., e.g. [14]. Fewer studies have been conducted on eventuality and consequences of an LH_2 BLEVE. A study [15] attempted to define a correlation to evaluate the flame volume produced by the ignition of the hydrogen-air mixture created from spillages of liquid hydrogen in the range 2.8 ℓ –89 ℓ. The flame volume was found to be proportional to the liquid hydrogen volume (ℓ) by a coefficient of 750. The authors published a correlation to define the height and width of a fireball as function of the mass m_{LH2} of liquid hydrogen:

$$H_{max} = W_{max} = 8.056\sqrt{m_{LH2}} \tag{6}$$

An updated correlation for fireball size based on work by [15] to best-fit experiments and calculate hazard distances for the scenario of liquid hydrogen storage tank rupture in a fire in the open atmosphere was suggested [16]. Analytical and theoretical models were proposed in [17, 18] to assess the consequences from BLEVE in terms of pressure and thermal hazards.

A series of experiments was conducted in 1996 investigating the potential hazards from rupture of LH_2 tanks [19]. Experimental tests employed a single wall tank with a volume of 120 ℓ. Totally ten tests were performed. Hydrogen mass was included in the range of 1.8–5.4 kg. Maximum pressure in the tank was 1.13 MPa. Tanks were ruptured by using a cutting charge along the tank circumference. Duration of the charge was about 2 ms and was deemed to not significantly contribute to the explosion. The patterns of the blast wave pressure dynamics varied from test to test depending on how the following different contributions verified in rapid succession or aggregately:

- Explosion of the cutting charge;
- Spontaneous vaporization of the liquid fraction after tank rupture and sudden expansion of gaseous hydrogen in the tank;
- Acceleration of flames and expansion of combustion products from the burning hydrogen/air mixtures.

A maximum overpressure of approximately 50 kPa was measured at 3 m distance from the tank. The maximum fireball diameter was between 6 and 15 m depending on the tank pressure. The maximum height achieved by the fireball varied between 16 and 20 m above the ground prior to extinction, which happened after about 4 s.

4.8 RPT phenomenon

An unintended release of liquid hydrogen on water may lead to a sudden and violent vaporization of liquid hydrogen, known as Rapid Phase Transition (RPT). Experimental work by Health and Safety Executive within the frame of PRESLHY project investigated whether rapid phase transitions and associated pressure effects are to be expected if water from sprinklers or hose jets is applied on liquid hydrogen in a tray with dimensions 800 × 800 mm × 100 mm. The experimental equipment (Figure 9) included pressure transducers to capture any overpressure produced and assess the verification of RPT.

Figure 9. Experimental facility for rapid phase transition investigation. Left: fully developed water spray from sprinklers. Right: water jet application into the centre of the tray (right).

Experiments carried out with the sprinkler systems showed that most of the vapour production was complete within approximately 30 seconds (Figure 10).

Figure 10. Vapor production after 5, 10, 20 and 30 s of water spray impingement.

For both sprinkler and water jet systems tests there was no significant recorded overpressure and no sign of rapid phase transition during the experiments. In the case of the test with sprinklers, there was significant formation and deposition of ice in the pool tray. Temperature records suggest there was an accumulation of condensed air at the bottom of the tray. On the contrary, at the end of test with the water jet there were no signs of ice in the pool tray. Presumably water displaced the liquid hydrogen so rapidly that there was no time for it to freeze. The tests showed an enhancement of the rate of vaporization of LH_2, which in case of ignition could result in severe consequences.

4.9 Purely cryogenic hazards

- **Material embrittlement**

Cryogenic temperatures on materials can reduce strength of structures up to irreversible failures.

- **Solidification of air components**

In case of LH_2 or cold H_2 releases, it could be possible that solid particles (water and CO_2 freezing) and/or LH_2 droplets and air condensate droplets (friction and break up) may ignite.

- **Extreme cold hazard**

Cryogenic liquids and their associated cold vapours and gases can produce effects on the skin similar to a thermal burn. Brief exposures that would not affect skin on the face or hands can damage delicate tissues such as the eyes. Prolonged exposure of the skin or contact with cold surfaces can cause frostbite. The skin appears waxy yellow. There is no initial pain, but there is intense pain when frozen tissue thaws.

Unprotected skin can stick to metal that is cooled by cryogenic liquids. The skin can then tear when pulled away. Even non-metallic materials are dangerous to touch at low temperatures. Prolonged breathing of extremely cold air may damage the lungs.

- **Asphyxiation hazard**

When cryogenic liquids form a gas, the gas is very cold and usually heavier than air. This cold, heavy gas does not disperse very well and can accumulate near the floor. Even if the gas is non-toxic, it displaces air. When there is not enough air or oxygen, asphyxiation and death can occur. Oxygen deficiency is a serious hazard in enclosed or confined spaces.

Small amounts of liquid can evaporate into very large volumes of gas. For example, one litre of liquid hydrogen vaporizes to 848 litres of hydrogen gas when warmed to room temperature.

5. Cryogenic release

The processes of release and subsequent distribution of a gas are strongly dependent on its thermodynamic state during storage. Pressurized gases form a free jet or will be flash released, if there is a complete failure of the storage vessel. For cryogenic storage, the substance will be liberated - depending on the leak location - as saturated vapor or as a liquid which starts to vaporize immediately. Parameters of concern are the expansion of a flammable vapor cloud, the height that it could attain, the time until it becomes sufficiently diluted below the flammability limits, and the total quantity of fuel in the cloud.

5.1 Single-Phase Releases

Experiments were carried out on releases of cryo-compressed hydrogen with temperatures 50, 200 and 300 K, and pressures up to 90 MPa [20]. Release diameter was in the range 0.2–1 mm. Results showed that for decreasing supply temperature, there is an increase in leakage flow rate and hydrogen concentration. The results of hydrogen distribution were used to build an empirical relationship to determine the 1% concentration distance based on the hydrogen mass flow rate.

Ulster University analysed the applicability of notional nozzle theory [21] in CFD simulations to predict concentration decay in cryogenic under-expanded jets (PRESLHY D3.2, 2021). The CFD model employed a RANS approach with realizable κ-ε model for turbulence. Simulation results well predicted experiments by [22] with release pressure up to 0.5 MPa and temperature in the range 50–61 K (Figure 11). CFD results showed that for the given scenario the presence of a co-flow of air to the jet did not affect the axial hydrogen decay. The extraction velocity at the hood was found to not affect results when varied in the experimental range 2–8 m/s.

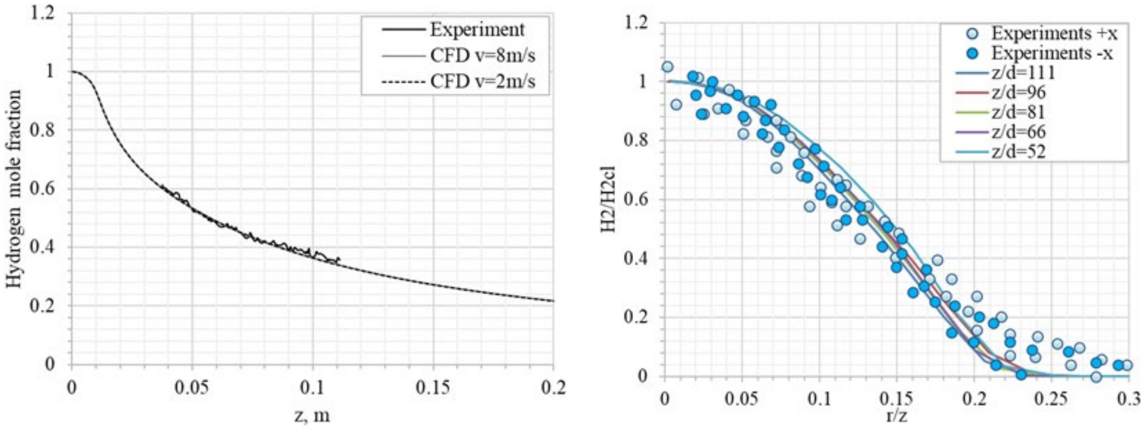

Figure 12. Hydrogen concentration along the jet axis (left) and normalized radial distance (right): simulation results versus experiments for test with $T = 61$ K, $P = 0.2$ MPa, and $d = 1.25$ mm.

The properties of the cryogenic flow at the nozzle can be significantly affected by heat transfer through the wall of a non-insulated pipe connecting the storage system to the nozzle. This was investigated numerically by Ulster University (PRESLHY D3.2, 2021) and results showed that even in a release pipe as short as 60 mm exposed to external ambient temperature air, the inclusion of heat transfer effect can cause a decrease of 9% of the hydrogen mass flow rate and significant variation of the flow temperature and properties at the nozzle.

5.2 Multi-Phase Releases

Experiments were carried out on cryogenic hydrogen choked releases through an elliptical converging-diverging nozzle with 2.934 mm throat diameter [23]. Examined hydrogen stagnation conditions were in the sub-cooled liquid regime. Pressures were in the range 1.29–5.89 MPa and temperatures in the range 27.2–32.3 K. The NASA experiments were used in several modelling studies to assess the capability of multiphase release models to predict the hydrogen mass flow rate and properties at the nozzle.

A Homogeneous Non-Equilibrium Flash Model (HNEM) was used [24, 25] which accounts for liquid superheat through a constant, prescribed "non-equilibrium" parameter. The approach implements the NIST EoS [26]. Calculations resulted in consistently larger mass fluxes than experimentally measured, but within a 10% variation. The Homogeneous Equilibrium Model (HEM) was used to model NASA releases [27, 28]. In this case, NIST EoS was also used and mass flow rate was predicted with a 10% accuracy.

6. Combustion

6.1 Cryogenic jet fires

6.1.1 Thermal loads

Several experimental studies were performed on thermal hazards from cryogenic hydrogen jet fires. In the work of Friedrich et al. [29] ignited hydrogen releases with absolute pressures up to 3.5 MPa and temperature in the range 34-65 K were analysed. Radiation level up to 10 kW/m^2 was recorded at 0.75 m from the jet fire. According to published harm criteria [30], a person standing at this distance would suffer second-degree burns if exposed for 20 s to the jet fire. Sandia National Laboratories (SNL) measured the radiative heat flux from cryogenic jet fires with release temperatures down to 37 K and pressures up to 0.6 MPa [31]. Experiments showed that for a same mass flow rate, the decrease of release temperature led to an increase of radiative heat flux. The flame length was seen to correlate well with the square root of the Reynolds number.

Saffers et al. [32] proposed a dimensionless correlation to determine flame length of both expanded and under-expanded hydrogen jet fires. The correlation was validated against jet fires with pressures in the range of 1–90 MPa and temperatures in the range of 187–300 K. Validation range of the correlation was further expanded in [33] to release temperature and pressure included in the ranges 46–295 K and 0.2–0.6 MPa, abs, respectively.

A selection of experiments by SNL [31] was used to validate a computational fluid dynamics (CFD) model to simulate flame length and radiative heat flux for cryogenic hydrogen jet fires with pressure up to 0.5 MPa, abs, and temperature in the range of 48–82 K [34]. The thermal dose for such jet fires was assessed in Ref. [34]. It was concluded that for all tests, at 0.5 m from the flame axis people should stand less than 30 s to not incur in first degree burns. Within the frame of PRESLHY project (PRESLHY D5.2, 2021), Ulster University extended the CFD model validation to horizontal cryogenic hydrogen jet fires with pressures up to 2 MPa by comparison with experiments performed by Breitung et al. [35]. The numerical results provided insights into the thermal hazards from horizontal jet fires and associated distances to "no-harm" levels for people. It was observed that the buoyancy of combustion products has a positive effect on the reduction of the "no harm" distance defined by temperature along the release direction. This decreased from $x = 3.5\times L_f$ for vertical jet fires to $x = 2.2\times L_f$ for horizontal jet fires (L_f being the flame length). Thermal radiation led to longer "no-harm" distances in the direction of the jet ($x = (3.0–3.2)\times L_f$) compared to a hazard distance defined by temperature. Ulster University developed a reduced tool to evaluate the radiative heat flux in the surrounding of hydrogen jet fires from vertical and horizontal releases of hydrogen at ambient and cryogenic temperature (PRESLHY D6.5, 2021). The reduced tool is based on the weighted multi source flame radiation model developed by [36] and further expanded by [37] for application to large scale flames. The radiative heat flux prediction depends on the evaluation of the radiant fraction

X, which is the ratio of the energy effectively emitted by the flame as radiation and the chemical energy associated to the fuel stream, based on the following correlation [38]:

$$X = 0.08916 \log_{10}(t_f \cdot \alpha_f \cdot T_{ad}^4) - 1.2172 \tag{7}$$

Ulster University adapted the model to include evaluation of flame length and width through the dimensionless correlation validated against cryogenic releases in Ref. [33] and expanded the validation range to hydrogen jet fires with pressure in the range 0.2–90 MPa and temperatures in the range 48–315 K.

6.1.2 Pressure loads from delayed ignition

Significant deflagration pressures may be created in case of a delay between the beginning of the release and ignition of flammable mixture in the highly turbulent hydrogen jet. Experiments on delayed ignition of releases at ambient temperature and 40 MPa spouting pressure generated an overpressure up to 20 kPa at 4 m distance [39]. Several experimental studies on ambient hydrogen releases demonstrated the dependency of blast wave overpressure on release conditions, i.e. pressure and orifice diameter, and ignition parameters, i.e. delay time and location [40, 41].

The study by Friedrich et al. [42] presents experiments on delayed ignition of hydrogen releases with pressure up to 3.5 MPa, release temperatures in range 34–65 K and nozzle diameters of 0.5–1.0 mm. Results showed that the maximum ignition distance was found for location corresponding to 7% by vol hydrogen in air. The maximum flashback distance was found for H_2 = 9% by vol, which is slightly lower than the distance for ambient temperature releases corresponding to 11%. During the tests, measured sound levels were recorded below 120 dB(A).

Within the frame of PRESLHY project, an engineering correlation was developed by partner UU to predict the maximum overpressure that could be produced by a hydrogen jet for a given storage pressure and release diameter (PRESLHY D6.5, 2021). The similitude analysis was applied to build a correlation. The dimensionless overpressure generated by delayed ignition of hydrogen jets at an arbitrary location, $\Delta P_{exp}/P_o$, is correlated to the dimensionless parameter composed of the product of the ratio of the dimensionless storage pressure, P_s/P_o, and the square of ratio of release diameter to the distance between the centre of the fast burning mixture in the jet (25–35% by volume) and the target location, $(d/R_w)^2$.

6.1.3 Pressure peaking phenomenon

The pressure peaking phenomenon (PPP) can be produced by hydrogen releases in confined spaces with limited ventilation. This is characterized by transient pressure dynamics with a distinctive peak exceeding the steady state pressure. The magnitude of the peak pressure depends mainly on hydrogen release rate, ventilation rate, and enclosure volume. Numerous experimental, analytical, and numerical works have been performed on PPP originated by releases of ambient temperature hydrogen [43- 49]. In the frame of PRESLHY project, the PPP for cryogenic hydrogen ignited releases in a garage-like scenario was investigated by partner Ulster University through numerical modeling (PRESLHY D5.2, 2021).

At a constant storage pressure (11.78 MPa) and a fixed release nozzle (4 mm), when the storage temperature decreases from 227 to 100 K, the released hydrogen increases from 11.37 to 23.16 g/s. As a consequence, the pressure peak increases from 20.86 to 42.82 kPa (almost doubled).

6.2 Liquid pool burning

6.2.1 Phenomenology

Regarding open burning pools of flammable liquids, the essential parameters are the burning rate and the temperature or heat flux distribution. For a burning gas cloud above a ground pool or tank, heat transport from the burning cloud to the pool is given by conduction, convection, and radiation enhancing the vaporization rate and the pool regression rate, respectively. The fire of a burning vapor cloud may also be able to travel back to the spill point and continue to burn as a pool fire. Hazards associated with pool fires are strongly depending on pool size and shape, burning rate, flame geometry, and heat radiation.

Two regimes for the regression rate have been identified depending on the pool dimension [8]. For small diameters (D < 0.2 m), heat transport by conduction is dominant, and the regression rate decreases with increasing radius (Figure 12).

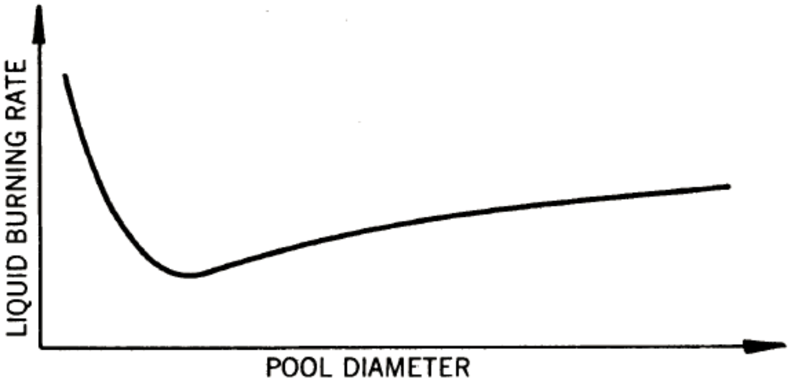

Figure 12. Qualitative liquid burning rate dependence on pool diameter [8].

Liquid hydrogen pool fires were observed to be dynamic and non-homogeneous with a highly intermittent pulsing structure of the flame. This cyclic changing of flame height is mainly due to the turbulent mixing of air and subsequent combustion and has an influence on the flame temperature. The height of the flame indicates the radiation hazard imposed by the fire, since it directly relates to the heat transfer from the flame into the surroundings. Usually, the flame height is defined as the height at which flame is present at least 50% of the time.

Effects of wind on the flame length are complex. For smaller pools, enhanced ventilation may improve air entrainment and thus allows for a more efficient combustion. Wind tilts the flame expanding the flame base area and changing the distribution of radiant heat flux distribution. This influence may even enhance the regression rate. For larger pools, measurements indicate enhanced burning rates. There is, however, a slight decrease for very large pools (D > 5–10 m) which could be explained by having several separate burning cells rather than one big pool fire [50, 51].

Another observation from LNG pool fires is that burning rates and flame heights of pools on water are by a factor of 2 higher than those of pools on solid ground [52]. This is explained by the higher heat transfer from the water into the pool due to the rapid interaction with the water and fragmentation of the pool increasing the heat transfer area. This effect tends to produce smaller pool diameters, but taller flames. The total radiation area is reduced, since a larger fraction of the vapor produced may escape unburnt from the plume.

6.2.2 Experimental work

From January 1958 to December 1959, Bureau of Mines, U.S. DOI experimentally measured the burning rates of LH_2 pools and compared the rates with other liquid fuels [8]. Figure 13 shows a comparison of the burning rates at steady state between LH_2 and liquid natural gas, which were measured in a 150 mm diameter Dewar[1].

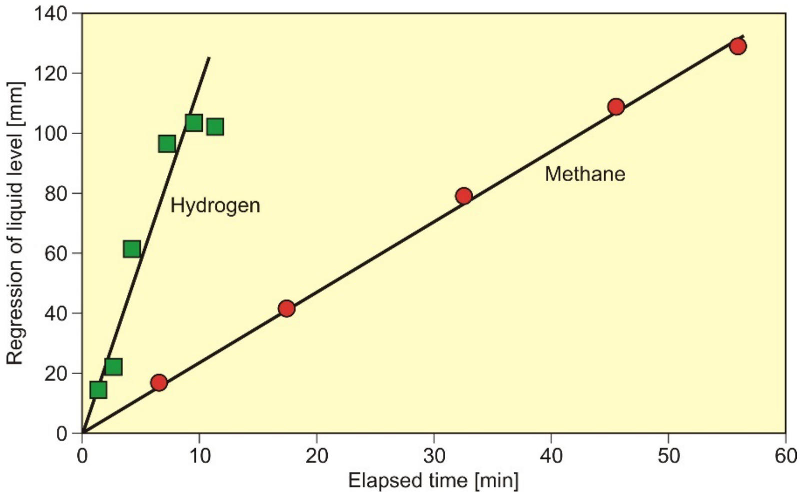

Figure 13. Steady-state burning rate comparison between LH_2 and LCH_4 [8].

For the LH_2 spill and ignition tests, with quantities of 54-90 ℓ given onto a steel plate or loose gravel, the overpressures were measured at a distance of ~50 m (see Figure 14). As shown in Figure 15, the blast pressures produced depend on the time delay for ignition [8]. The blast pressure initially increases with delay time, until 5–6 s of delay, then decreases when the H_2 concentration in the rising and diffusing vapor clouds became smaller.

---

[1] a double-walled flask of metal or silvered glass with a vacuum between the walls, used to hold liquids at well below ambient temperature.

Figure 14. Ignition of the LH_2 vapor cloud during low wind conditions (no secondary explosion).

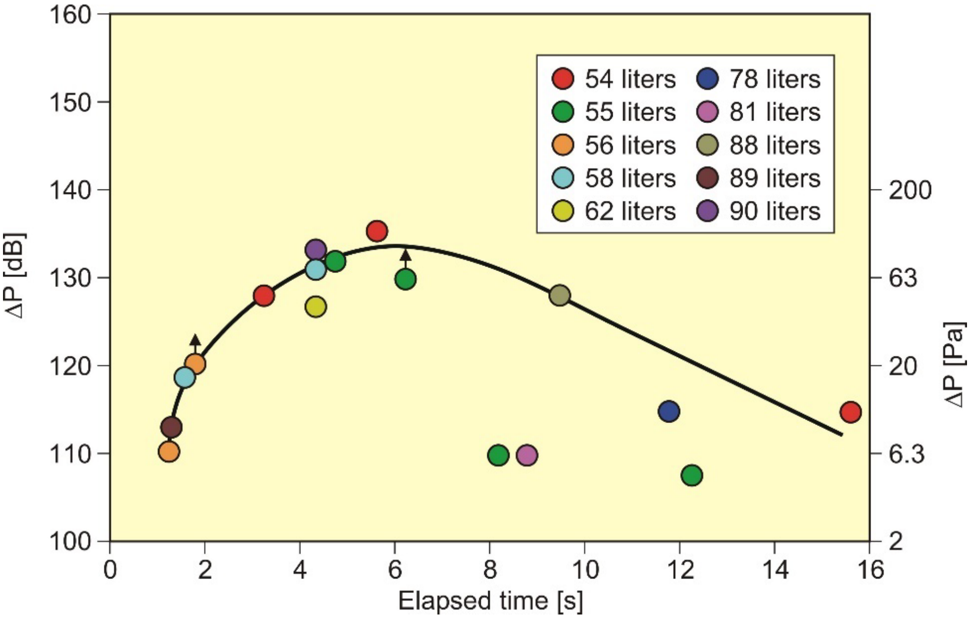

Figure 15. Overpressures measured at 49 m distance after ignition of vapor cloud above LH_2 pools vs. time of ignition after spillage [8].

Longer ignition delay allows the build-up of larger flammable cloud and reproduces the liquid/solid pooling phenomena during unignited releases of LH_2 [53]. The extent of the flammable cloud appeared to be congruent with the extent of the visible water vapor cloud created by the very cold hydrogen cloud. The flame speeds were from 25 m/s up to 50 m/s with increasing release duration.

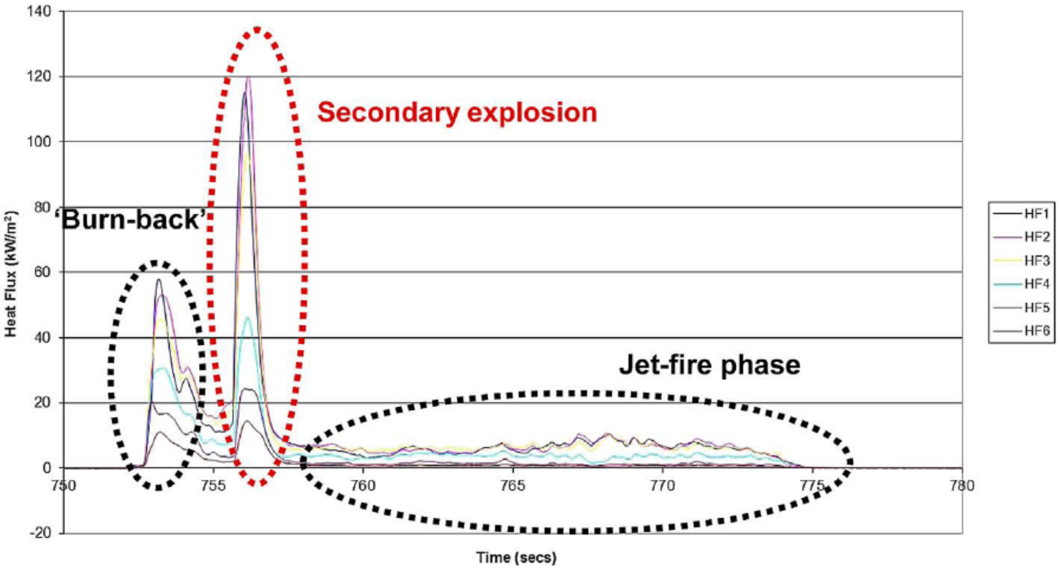

Figure 16. Radiometer readings from ignited release exhibiting a secondary explosion.

On one occasion, when the flammable cloud was ignited, it burnt back to source, creating a jet fire and then a secondary explosion emanated from the liquid/solid pool location. The separate phases of the burning cloud are highlighted in the radiometer plot from the test, shown in Figure 16. The first peak on the plot represents the initial deflagration of the cloud back to the release point or "burn-back"; the second, larger peak represents the secondary explosion and the longer radiative phase after represents the resulting jet fire.

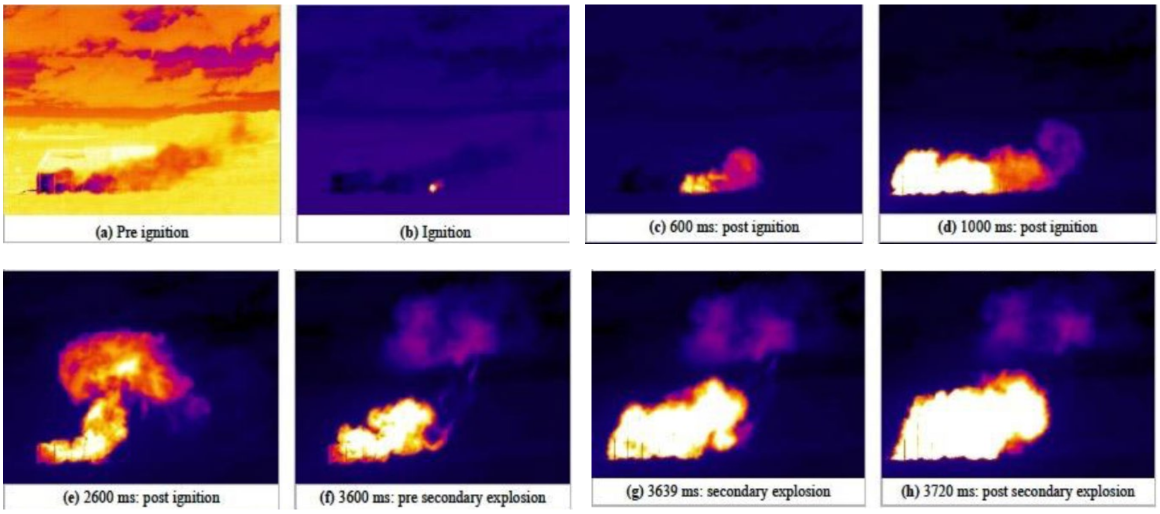

(a) Pre ignition

(b) Ignition

(c) 600 ms: post ignition

(d) 1000 ms: post ignition

(e) 2600 ms: post ignition

(f) 3600 ms: pre secondary explosion

(g) 3639 ms: secondary explosion

(h) 3720 ms: post secondary explosion

Figure 17. IR video stills of Test 6 including secondary explosion.

In Test 6, ignition occurred from igniter no. 3 and propagated back through the horizontal cloud towards the release point. The flame front accelerated up to speeds of 50 m/s and began to lift upwards once momentum was lost. A jet of flame continued to burn from the release point after the vapour cloud had been consumed as in the previous test. However, approximately 3.6 s after the initial cloud ignition, a secondary explosion occurred emanating from the liquid/solid pool location (Figure 17, images f–h). This secondary explosion created an 8 m diameter hemispherical fireball around the solid/liquid pool location and created a noise level audible from over a mile away. Following the secondary explosion seen in Test 6, further tests were performed to try to replicate this phenomenon. However, the meteorological conditions during other tests were different from Test 6 and no secondary explosion could be replicated.

The experimental evidence of the past 50 years [15, 54-59] illustrates that even very large spills of LH_2 do not create lasting hazardous situations that are typical to hydrocarbons spills. The thermal load generated by an LH_2 pool fire is about 3–3.5 times lower than that of equal-size hydrocarbon pools.

There is no propensity to detonation either in the open environment. The most hazardous phenomenon develops when solidified air is becoming enriched with oxygen and then gets into contact with a burning (otherwise relatively mildly) hydrogen plume or jet. From this perspective, a secondary explosion induced by solid oxygen-enriched air (as was registered by HSL in their test 6) appears to be a more hazardous event than a BLEVE (considering a LH_2 spill and a BLEVE occur on an equal size tanker).

A BLEVE that would result in a tank failure and instantaneous spill of all LH_2 inventory, will, of course, freeze surrounding air. But, since the amount of LH_2 will be dominant (vs. a spill that develops gradually), this solid air will not have time to get enriched with oxygen and, since it is heavier than LH_2, it will be covered by the vaporizing liquid. We know from the NASA and ADL experiments that whether the liquid is ignited or not, it does not affect LH_2 pool evaporation or its regression rate. As was shown by Urano [58], the only real accelerant is the contact with solid air enriched with oxygen. But since under BLEVE condition it is covered by the liquid hydrogen, it is not involved in the combustion until most of the liquid has vaporized and risen to the atmosphere. Hence, solidified air would only affect a relatively small quantity of hydrogen and since it is not oxygen-enriched, an “explosion” (which would be a fast deflagration) is unlikely as was shown by the HSL experiments.

The unignited HSL test performed at 86 cm above ground demonstrated that it does not result in solidification of air. It is possible that some sort of air “rain” or droplets might be present in the jet. However, due to moisture content in the air that condenses together with air in the cold hydrogen plume, the potential for oxygen enriched air is significantly reduced, if not completely eliminated. In this case, a secondary explosion would not be possible. However, because the hydrogen plume is high enough above the ground and thus free from friction, it may travel farther than the vaporizing cloud from the LH_2 pool. Hence, this scenario presents a new condition worth analysing separately.

Finally, the recent analysis of unignited experiments by HSL has shown that the gas-liquid slurry coming out of release orifice is a two-phase fluid even before it reaches the orifice. Calculations suggested that the gaseous component at the exit is 96% by volume and 31% by mass, respectively. This indicates that analysing (cold) hydrogen gas leaks is as relevant as analysing liquid leaks.

6.3 Deflagration of cold hydrogen-air mixture

Within the flammability limits, three flame propagation regimes can be distinguished for gaseous mixtures:

- slow subsonic deflagrations ($v < c_r$ - flame velocity v is less than the speed of sound in reactants c_r);
- fast supersonic flame ($c_r < v < c_p$ - flame velocity is less than the speed of sound in products c_p, but more than the speed of sound in reactants);
- detonation ($v = D_{CJ}$).

Figure 18 shows the possible regimes for hydrogen-air mixtures at initial pressure 0.1 MPa. Mixtures with expansion rate σ lower than the critical expansion rate σ* cannot accelerate effectively and only subsonic combustion regime may occur. In such case, characteristic pressure loads are in the range 0.1–0.2 MPa for an initial pressure of 0.1 MPa. Mixtures with σ > σ* can effectively accelerate and detonate if condition $L > 7\lambda$ is verified, where L is the characteristic size of combustible domain and λ is the detonation cell size. In these cases, the characteristic pressure loads can vary from 0.6-0.8 MPa for sonic flames, to 2–4 MPa for detonation.

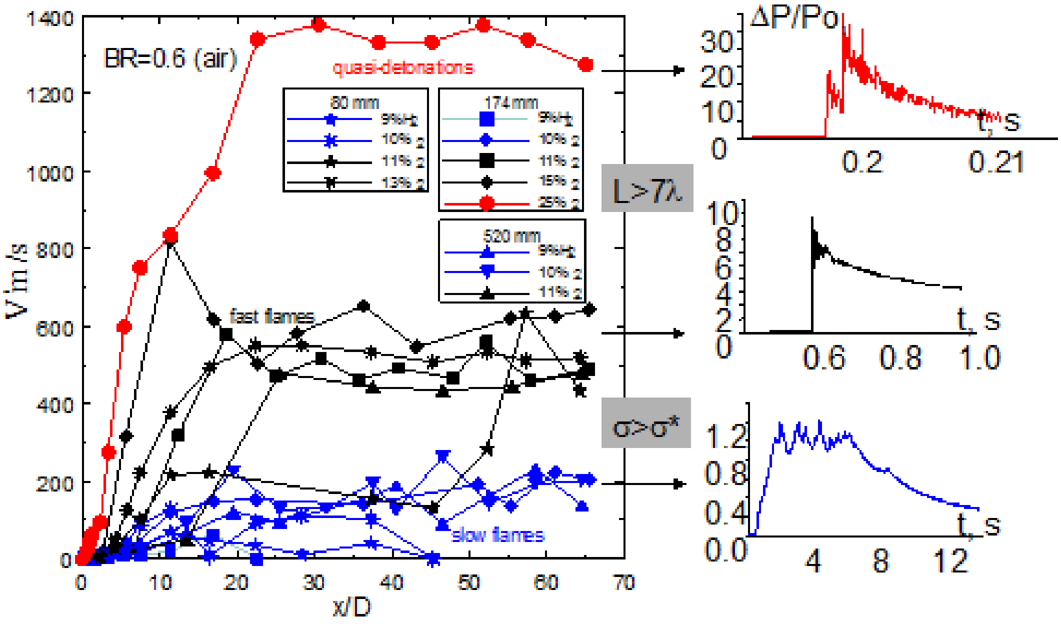

Figure 18. Combustion regimes for different hydrogen-air mixtures (P = 0.1 MPa, T = 293K): right pictures correspond to pressure signals for different regimes [60, 61].

The critical expansion ratio σ* decreases with initial temperature T_u increase and overall energy activation E_a decrease (E_a/T_u decreases) (Figure 19).

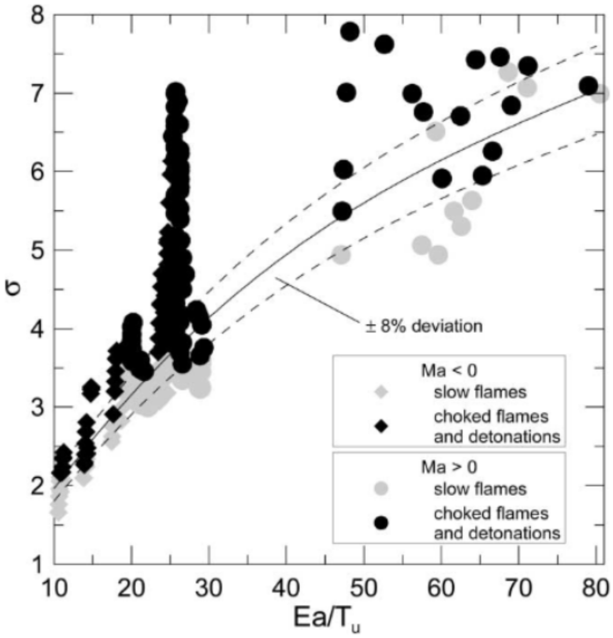

Figure 19. Resulting combustion regime as a function of expansion ratio σ and dimensionless effective activation energy, E_a/RT_u, for mixtures of hydrogen and hydrocarbon fuels [60].

Figure 20 (left) shows the extrapolation to cryogenic mixtures of the critical expansion ratio σ*. Figure 20 (right) reports the threshold of H_2 concentration by mol to obtain flame acceleration to flame speed higher than speed of sound. It could be observed that this limit decreases from 11 to 9% with decrease of temperature from 300 K to 78 K.

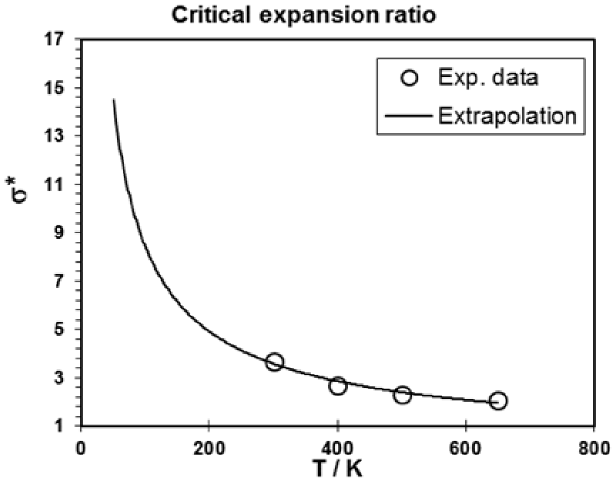

T, K	C_{H_2}, %mol	σ*
300	11	3.75
200	10.34	4.92
150	10.09	6.14
100	9.58	8.49
78	9.13	10.67
50	8.60	13.89

Figure 20. Critical mixture expansion ratios versus initial temperature: extrapolation to cryogenic temperatures (solid line) [60].

Within the frame of PRESLHY project, HSE carried out an extensive experimental campaign to assess the effect of congestion or confinement on an ignited hydrogen cloud stemming from a release of LH_2, potentially leading to deflagration to detonation transition (DDT). Experimental measurements included overpressure, heat flux, and noise levels. A total of 23 ignited trials were conducted on LH_2 releases from a tanker with pressure of 1 or 5 barg and through nozzle diameters equal to 6 mm, 12 mm and 25.4 mm.

The congestion and confinement were created by a configurable steel structure placed directly in the path of the release. Results showed that the increase in volumetric congestion increases the measured overpressures in releases with the same initial conditions. In case of densely congested area with a volume blockage ratio and volume larger than 4% and 15 m^3, respectively, it could be reasonable to assume that a high-level explosion or DDT may occur. The results also showed that an increasing hydrogen inventory, either through an increased release pressure or larger nozzle, can result in a larger event upon ignition. It was observed that the ambient conditions, in particular the wind speed and direction, were a significant factor in the outcome of each ignition (Figure 21).

Figure 21. Pictures showing sudden gust immediately prior to ignition for test with release: $p = 1$ bar, $d = 12$ mm, and wind velocity = 2m/s.

7. Liquid hydrogen technology

7.1 Liquid hydrogen production process and infrastructures

One of the challenges in building a hydrogen economy is the establishment of an efficient production and supply infrastructure. Large scale distribution favours the relatively dense liquid phase LH_2, but liquefaction still suffers from low energy efficiencies. Historically, LH_2 was mainly used as a rocket fuel, where the low efficiency in the production did not matter. A major program of hydrogen liquefaction was started in the USA within space programs leading to the design and construction of large-scale liquefaction plants.

The liquefaction of H_2 is a highly energy intensive process. The minimum work required for the liquefaction of hydrogen (at ortho-para equilibrium) is 3.92 kWh of electricity/kg of H_2 or 0.12 kWh /kWh of H_2. Typical values for the whole process, however, are in the range of 8 - 14 kWh/kg for relatively large liquefaction units. Reducing the energy consumption of liquefiers is an active subject of development for the LH_2 industry (see IDEALHy FCH JU project for instance).

Large scale installations are typically implemented with a Claude process with LN_2 pre-cooling providing acceptable efficiencies, at least for the past main application as rocket fuel. The complete process comprises an initial purification unit, additional external coolers with helium or mixed refrigerants as operating medium. The expansion is split in up to 6 stages and several ortho-para converters are integrated. All cold parts are mounted in a cold box, which is thermally insulated for instance with perlite.

Worldwide there are nearly 30 large scale liquefiers in operation with production capacities from 1 to ~35 t/d of LH_2 in a unit (see Figure 22 for instance). Most and with the largest capacities are installed in the USA. In the European Union and in Asia, particularly Japan, H_2 liquefaction capability is existing and on the rise. Additionally, there are several laboratory-scaled liquefiers in operation with a capacity of a few kg/day [62]. A list of currently operated liquefaction plants in the world is given in Table 3. Moreover, Table 4 contains a list of liquefaction plants that were found to be under construction or planned to go into operation in near future.

Figure 22. Air Liquide LH_2 filling stations (left: Little Town, USA; right: Becancour, Canada).

Table 3. Operating commercial hydrogen liquefaction plants in the world.

Place	**Operator**	**Capacity (t/d)**	**Operation since**
		Europe	
Rozenburg, Netherlands	Air Products	5.0	1987
Wazier/Lille, France	Air Liquide	10.5	1987
Kourou, French Guiana	Air Liquide	2.5	1990
Ingolstadt, Germany	Linde	4.5	1992
Leuna, Germany	Linde	5.3	2007
Total Europe		**27.8**	
		America	
Ontario, CA	Linde-Praxair	20	1962
New Orleans, LA	Air Products	34 + 34	1977
Niagara Falls, NY	Praxair	38	1981/1989
Sarnia, ON	Air Products	29	1982
Bécancour, QU	Air Liquide	11	1986
Montreal, QU	Air Liquide	10	1986
Sacramento, CA	Air Products	5	1986
Magog, QU	Linde	15	1990
Pace, FL	Air Products	29	1994
McIntosh, AL	Praxair	24	1995
East Chicago, IN	Praxair	30	1999
Total America		**279**	
		Asia	
Beijing, China	CALT	0.6	1995
Mahendragiri, India	ISRO	0.3	1992
India	Asiatic Oxygen	1.2	
India	Andhra Sugars	1.2	
Ooita, Japan	Pacific Hydrogen Co.	1.9	1986
Kimitsu, Japan	Nippon Steel Corp.	0.2	2004
Sakai (Osaka), Japan	Hydro Edge Co., Ltd.	5.1 + 5.1	2006
Ichihara (Chiba), Japan	Iwatani Industrial Gases Corp	5.1	2009
Shunan (Yamaguchi), Japan	Yamaguchi Liquid Hydrogen Corp	5.1	2013
Harima (Akashi), Japan	Kawasaki Heavy Ind.	4.2	2015

Baikonur, Kazakhstan	Cryogenmash	4 – 17	~1960
Plesetsk, Russia			
Total Asia		**~47**	
Total World		**~355**	

Table 4. Commercial hydrogen liquefaction plants in the world under construction/planning.

Place	**Operator**	**Capacity (t/d)**	**To be onstream in**
Leuna, 2nd plant	Linde	5	2021
Carson, CA	Air Products	10	2021
La Porte, TX	Air Products	~28	2021
Las Vegas, NV	Air Liquide	30	2022
USA	Chart Industries	14 + 14	2022
Haiyan/China	Air Products	30	2022
Weinan, China		8.5	
Chubu Pref, Japan	Ituchu-Air Liquide	30	~2025
Ulsan, ROK	Hyosung/Linde	35.6	
Changwon, ROK	Doosan Heavy Ind. / Air Liquide	5	2023
Total		**~210**	

Note that Table 3 and 4 are available in Deliverable 6.1 – Handbook of hydrogen safety: Chapter on LH_2 safety. Pre-normative REsearch for Safe use of Liquid Hydrogen (PRESLHY). The specific energy consumption, A, of today's hydrogen liquefiers is in the order of 12-15 kWh/kg of LH_2, 3 to 4 times higher compared to the minimum energy required (3.9 kWh/kg). This corresponds to an exergy efficiency (A_{min}/A) in the range of 25–33%. Target value for an optimized liquefier design is 6.2 kWh/kg [63]. Improvement in efficiency is expected with the development of new materials and new compression/expansion technology. As an example, the recently established plant in Leuna, Germany, indicates a specific energy consumption of 10.3 kWh/kg (feed compression excluded) [64].

7.2 Liquid hydrogen storage and transport

7.2.1 Liquid hydrogen storage

Liquid hydrogen storages are already existing for professional for long time ago. But up to now there is no liquid hydrogen storage in public domain. Storage tanks for LH_2 can hold more hydrogen compared to those for GH_2: volumetric capacity of LH_2 is 0.070 kg/L as opposed to 0.030 kg/L for GH_2 tanks at 70 MPa. However, a significant amount of energy (around 30% of the energy contained in hydrogen) is required for liquefaction. Hydrogen may be liquefied for a simplified transport or storage. All of the major industrial gas suppliers have cryogenic delivery tankers. LH_2 is used at hydrogen refuelling stations and in airspace applications.

The volume expansion ratio of LH_2 to GH_2 is 848. LH_2 is stored at low (cryogenic) temperatures and at pressures of around 0.6 MPa. An appropriate and sufficient level of tanks insulation is needed to prevent the release of evaporated gas. The costs of materials suitable for LH_2 storage tanks as well as the volumes and weights of tanks are significantly higher than those for GH_2.

The LH_2 storage tank is a Dewar, double-walled, vacuum-insulated vessel made of lightweight steel alloys. There is no permeation, as the double-walled tank retains vacuum between the walls. The LH_2 storage has a major challenge. The inherent heat input from the environment may lead to warming and boiling of LH_2 inside the tank. When the pressure in the storage vessel remains constant the vapours produced from boiling of LH_2 are called boil-off. These vapours can be released through venting. The boil-off (evaporation of LH_2) can be caused by the following factors:

- *Ortho- para-hydrogen conversion*: conversion of ortho- to para-hydrogen is an exothermic reaction. If the unconverted normal hydrogen is placed in a storage vessel, the heat of conversion will be released within the container, which leads to the evaporation of the liquid.
- *Residual thermal leaks*: the heat leakage losses are proportional to the ratio of surface area to the volume of the storage vessel. The shape of cryogenic vessel should be spherical since it has the least surface to volume ratio. A big cause of heat leaks in cryogenic storage is through the support struts in the vessel.
- *Sloshing*: a motion of LH_2 in a vessel due to acceleration or deceleration, which occurs during its transportation by tankers. Some of the impact energy of the liquid against the vessel is converted to thermal energy.
- *Flashing:* occurs when LH_2 at a high pressure is transferred from trucks and rail cars to a low-pressure vessel.

The main components of on-board LH_2 tank are shown on Figure 23. They include:

- LH_2 storage container,
- Shut-off devices,
- A boil-off system,
- Thermal-activated Pressure Relief Devices (TPRDs),
- The interconnecting piping (if any) and fittings between the above-mentioned components.

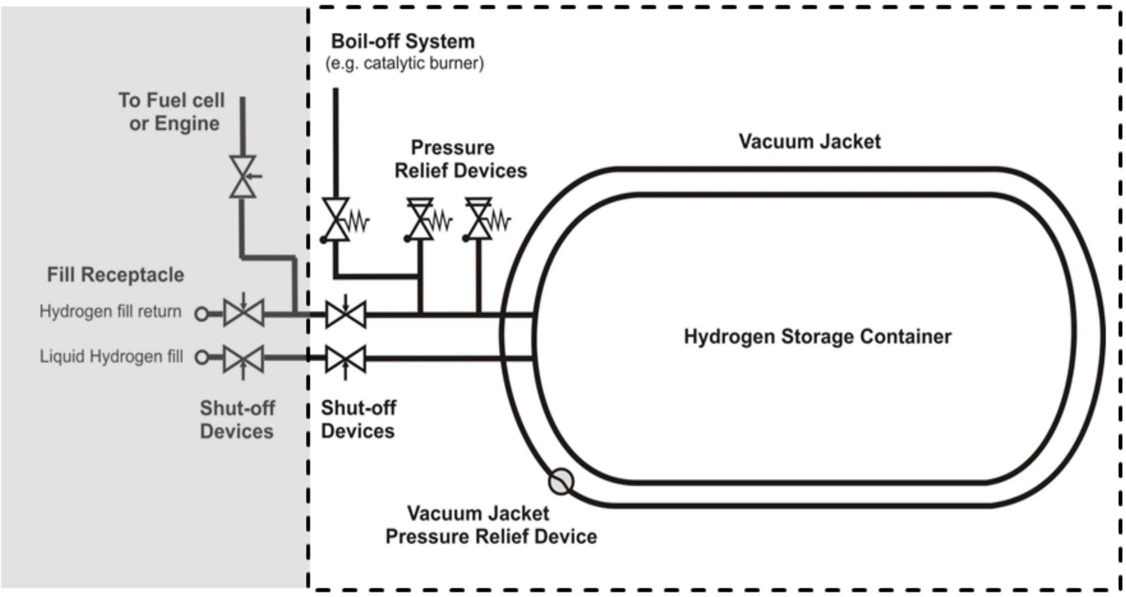

Figure 23. A schematic representation of LH_2 storage system from Ref. [65]

Some safety issues associated with LH_2 storage are discussed below:

1. A loss of LH_2 containment. A damage of the external tank walls can lead to the disruption of vacuum, causing heating and subsequent pressure rise inside the vessel. This should be avoided wherever possible.
2. Formation of oxygen-enriched atmospheres. The condensed air may form oxygen enriched atmospheres in the vicinity of LH_2 storage. The solid deposits formed by condensed air and LH_2 could be enriched with oxygen. This poses a risk of explosion if the external wall tank is damaged. The mechanism is considered as a possible reason for a powerful secondary explosion occurred during large-scale LH_2 release experiments at HSL [66].
3. The boil-off. It raises concerns when vehicles are parked for a long time as the pressure build-up is possible until the boil-off valves open.
4. Ice formation. Low temperatures may result in ice build-up on the storage elements (e.g. valves, Dewar's) leading to an excessive exterior pressure, and to a possible rupture of the vessel.

Cryo-compressed storage combines storage of hydrogen at cryogenic temperatures in a vessel that can be pressurised (e. g. to 35 MPa), as opposed to current LH_2 vessels which employ near-ambient pressures. Liquid hydrogen or cold compressed hydrogen can be stored. This technology, which is still at R&D stage, was developed by Lawrence Livermore National Laboratory (LLNL) and BMW Group. It has the following advantages:

- higher hydrogen density compared to LH_2 and GH_2 storage options;
- potential improvement in weight, volume and overall costs of tanks;

- significantly lower theoretical energy of cryogenic hydrogen associated with tank rupture;
- lower evaporative losses than liquid hydrogen and the tanks are much lighter than metal hydrides.

These storages can be in vertical or horizontal position. Cryogenic fixed storage has a volume from 10 m^3 to 300 m^3 with an internal pressure around 12 bar.

Figure 24. Horizontal and vertical liquid hydrogen storages. (Source Air Liquide).

In order to manage storage at -253°C, for large storage (> 100 m^3 water volume) double-walled vacuum insulated pressure tanks are used. Such vessels consist of an inner pressure vessel, an external protective jacket and compressed perlite under vacuum in the space between the inner vessel and the outer jacket. Perlite is an inorganic amorphous volcanic glass that represents a good trade-off between cost and insulation properties. For smaller storages (< 100 m^3), single-walled pressure tank with multi-layer insulation coating is used.

In most of the cases, LH_2 storages are aerial. Nevertheless, it exists few cases of underground LH_2 storages, buried or vault as illustrated and defined in Figure 25.

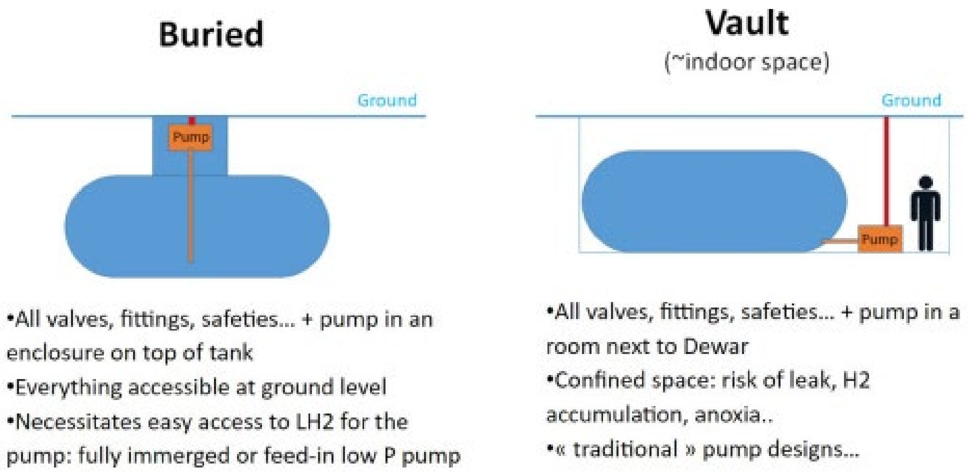

•All valves, fittings, safeties… + pump in an enclosure on top of tank
•Everything accessible at ground level
•Necessitates easy access to LH2 for the pump: fully immerged or feed-in low P pump

•All valves, fittings, safeties… + pump in a room next to Dewar
•Confined space: risk of leak, H2 accumulation, anoxia..
•« traditional » pump designs…

Figure 25. The two main possible designs for underground LH_2 storages.

"Buried" design has safety advantage but necessitates an immersed LH_2 pump (low or high pressure), that is a technology not very well mastered. "Vault" design keeps the earth/fill away from direct contact with the system using a wall. It does not have any technical barriers, but has limitations in terms of safety (leaks, anoxia), and possibly higher civil work cost.

Table 5. List of known underground liquid hydrogen storages.

Year	Location	Design	Station operator
2004	Washington DC	Vertical, in a sleeve	Shell
2005	London	Vault	BP
2007	Munich	Vault	Total
2010	Berlin	Vault	NA

7.2.2 Cryostat for stationary applications

Cryogenic vessels have been commonly used for more than 70 years for the storage and transportation of liquid hydrogen. Similar as for compressed storage there are two main classes of the LH_2 storage vessels. There are cryostats for stationary and for mobile applications. The vessel shown in Figure 26 is the world's largest LH_2 tank located at the NASA Kennedy Space Center (KSC) in Florida. The tank is a 3800 m^3 (3218 m^3 of LH_2) double-wall vacuum perlite (1.3 m of thickness) insulated spherical (in/ex diameter = 18.75 / 21.34 m) storage vessel. The tank is operated at a pressure of 0.62 MPa and has a boil-off rate of 0.025%/d.

Figure 26. LH_2 storage vessel with 3800 m^3 capacity at KSC in Florida (Source NASA).

In order to manage storage at -253°C, for large storage (> 100 m^3 water volume) double-walled vacuum insulated pressure tanks are used. Such vessels consist of an inner pressure vessel and an external protective jacket. The volume between inner vessel and jacket is filled with compressed perlite under vacuum. Perlite is an inorganic amorphous volcanic glass that represents a good trade-off between cost and insulation properties.

Although many large-scale tanks are of spherical shape to minimize heat loss to the outside, the LH_2 tanks at production sites are typically horizontally arranged. At the Kourou Ariane launch site in French Guiana, Air Liquide operates five semi-mobile tanks of 320 m^3 each (0.39 MPa) and one tank of 110 m^3 (1.1 MPa). Total capacity is 22 t. Another example shown in Figure 27 are the LH_2 storage tanks at the liquefaction plant in Waziers/France (Liquefaction unit = 10 t/d), AL operates four horizontal tanks of 250 m^3 each (in/ex diameter = 4.02 / 5.1 m - perlite thickness = 500 mm).

Figure 27. LH_2 stores at the Waziers liquefaction plant.

Modern tanks for liquid hydrogen production reduce boil-off losses to a minimum [67]. Nevertheless, it is assumed that roughly 1% of the liquid hydrogen will be lost due to boil-off per day during hydrogen storage at the refuelling station [68]. An average storage period of approximately three days is assumed.

For smaller storages (< 100 m^3), also single-walled pressure tank with multi-layer insulation coating are used (so-called MLI). This technology is described in more detail in Section 6.2.4 – liquid hydrogen transport.

7.2.3 Cryostat for mobile applications

The heat absorption for the small automotive cryostat shown in Figure 28 with an internal volume of about 100 ℓ is so reduced to about 1 W. This heat input leads to evaporation and via a pressure limiting valve to the boil-off. The boil-off corresponds to a loss of 1.5% of the stored energy per day for small cryostats. Thus, the typical stored mass of about 7 kg will be lost in two months if the car were not used in this phase.

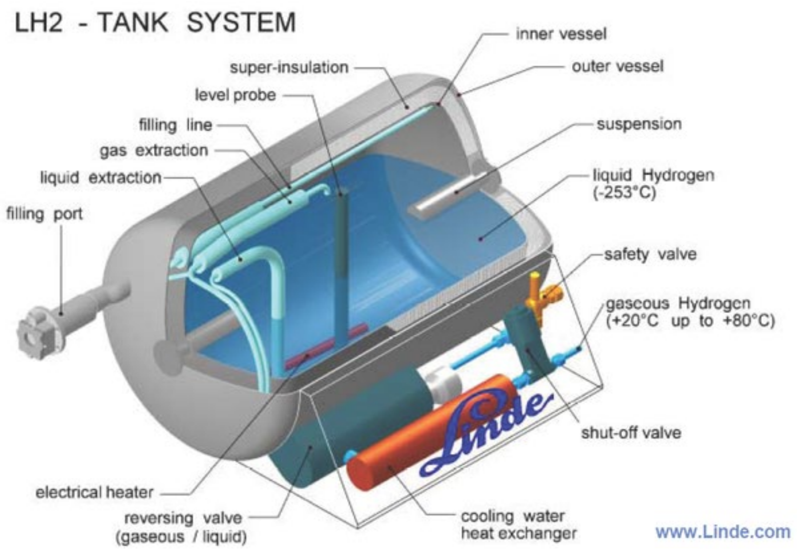

Figure 28. Schematic presentation of an LH_2 tank for automotive application (BMW 750h) produced by Magna Steyr (Source: Linde).

The boil-off management may reduce these losses or at least reduce the associated risk with released hydrogen by

- cold combustion with air in catalytic recombiners
- storing the boil-off gases in metal hydride storages
- re-cycling in a re-liquefaction
- direct energetic use, in a fuel cell for instance.

There is no doubt that the involved temperatures are demanding not only regarding the design of the actual storage but also regarding the compatibility of all connected technologies, like measurement techniques, armatures, valves, piping.

7.2.4 Liquid hydrogen transport

Depending on the scale and the desired use, hydrogen batch transport is based either on compressed or liquid hydrogen. Despite the higher efficiencies rooted in the higher densities of LH_2, in most cases high-pressure gaseous hydrogen is preferred over liquid hydrogen. This is because of the small numbers of liquefiers available worldwide and the higher energies required for liquefaction. So typically for long distance transport liquid hydrogen is the preferred option.

7.2.4.1 Road transport

Road transport of gaseous hydrogen is presently carried out using trucks with steel cylinders of up to 90 ℓ at 20–30 MPa pressure or large seamless cylinders called “tubes” of up to 3000 ℓ at 20–25 MPa. For transport at a larger scale, pressures of 50–60 MPa or even higher may be employed. A 40 t truck carrying compressed hydrogen can deliver only 400 kg because of the weight of the 20 MPa pressure vessels.

Over longer distances, road transportation of liquid hydrogen is more attractive than gaseous hydrogen. Cryogenic liquid hydrogen trailers can carry up to 5000 kg of hydrogen and operate up to 1.2 MPa. Hydrogen boil-off can occur during transport despite the super-insulated design of these tankers, potentially on the order of 0.5%/d. Hydrogen boil-off up to roughly 5% also occurs when unloading the liquid hydrogen on delivery.

The LH_2 tanks on the trailers are insulated using a vacuum super insulation. This insulation is also used for transfer piping systems (Vacuum MLI Insulated Piping). The Vacuum Super Insulation is a system of thermal insulation which includes:

- A double-shell insulation space (interspace) where static or dynamic (for large storage) high vacuum is limiting heat transfer by conduction and convection.
- A blanket of alternate layers of highly reflecting shields (aluminum for instance) and insulating spacers (Lydall for instance) to prevent heat transfer by radiation as well as conduction between shields.
- An adsorbent (molecular sieve) placed in the vacuum space in order to achieve an adequate level of vacuum at low temperature by adsorption of residual gases and moisture.

Two examples for LH_2 trailers as shown in Figure 29 are rather limited by the maximum dimensions of the transport vehicles. They come typically with a weight of ~25 metric tons for the empty tank plus a load of 2–3 t of LH_2.

Figure 29. Examples of LH_2 road truck transportation [69].

7.2.4.2 Pipeline transport

Similar to the extensively installed natural gas networks, the transportation of hydrogen at high pressure through pipeline systems has been realized already at a broad scale. In contrast, pipeline transportation of liquid hydrogen is existing at a small scale only. Pipes for transferring cryogenic liquid hydrogen must comply with the extreme low temperature of LH_2 and the associated insulation requirements. Similar to LH_2 storage tanks, pipelines are of double-wall design and vacuum-jacketed. A prototypical transfer pipe for LH_2 therefore consists of at least two concentric tubes combined with superinsulation material in the vacuum space. Stainless steel is usually taken for the inner line with low heat conduction spacers as a support in the vacuum jacket. Because of the high cost increasing linearly with distance LH_2 pipelines are economically attractive only for short distances. The transfer is done by pressure difference rather than by pumps. There are rigid or flexible variants. Major concerns, apart from heat leakage, are the mechanical stress imposed on the inner line due to contraction/expansion, pressure oscillations upon cool-down, or two-phase flow. Therefore, cryogenic pipes must be sufficiently flexible which can be done by appropriate pipe routing and expansion joints.

During the period of chill-down of an LH_2 line, a two-phase flow develops which is stratified for horizontal flows as is schematically shown in Figure 30, exhibiting a vapor layer above the liquid due to vaporization and a thin film underneath the liquid layer [70]. This phenomenon is encountered particularly in refuelling lines where chill-down is required before the fuelling process itself begins to avoid the gaseous phase to enter the tank.

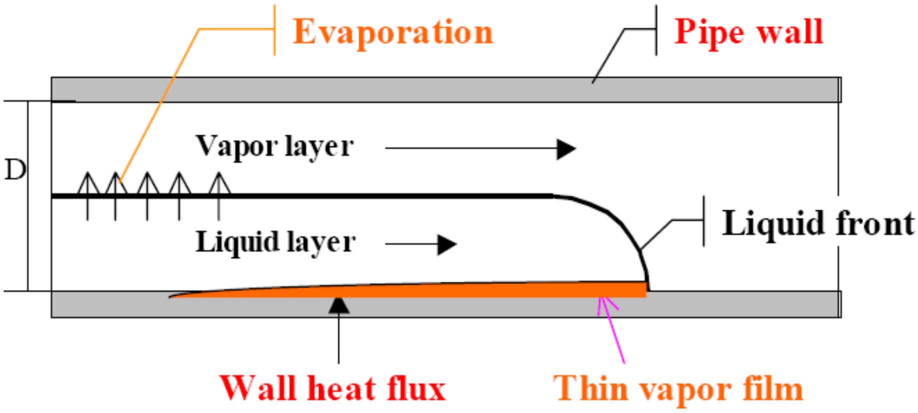

Figure 30. Two-phase flow in a horizontal line [70].

Figure 31 shows test and operations support contract engineers and technicians at the NASA Kennedy Space Center inspect an LH_2 supply hose at Launch Pad 39B. They are reviewing procedures preparing for a fit check of the new LH_2 transfer flex hose from its supply truck to the LH_2 tank at Pad 39B to confirm that the hose fits and functions properly.

Figure 31. Inspection of an LH_2 supply hose at NASA's Kennedy Space Centre (Photo credit: NASA/Frankie Martin).

The space centre's Ground Systems Development and Operations Program is overseeing upgrades and modifications to Pad 39B processing facilities to ensure all is in readiness to support Exploration Mission 1, the first flight of Space Launch System rocket and Orion space craft, currently planned for November 2021. Both are being developed for NASA's Journey to Mars.

For transferring LH_2 via pipeline from one storage to another (for instance from a large stationary storage to a truck or from a trailer to a storage tank at user's site), there are two methods:

- pressure buildup (natural pressure build up or voluntary vaporization of LH_2 via a small external heat exchanger). Hence, the pressure in the "mother storage" becomes more than the pressure in the "daughter storage" and LH_2 transfer is easy. The main drawbacks of this method are a long operating time and an increase of the pressure of the "mother" storage leading sometime to the need of a pressure venting;
- pumping in the "mother storage" using an appropriate transfer centrifugal cryogenic pump. The main drawbacks of this method are the cost of the pump and the need of frequent maintenance of the pump mostly due to cavitation (low available NPSH - Net Positive Suction Head: difference between liquid pressure and saturation vapour pressure of the considered compound - due to low density of LH_2).

At an LH_2 based hydrogen fuelling station, the LH_2 is typically delivered by an LH_2 truck. This LH_2 truck is composed of a 40 m^3 horizontal tank operating between 0.1 and 1.2 MPa. The connection between the storage and the truck is done by a flexible transfer line (Figure 33). The transfer is performed without a pump. A small vaporizer is present on the trailer to produce a pressure build up in the truck tank and to allow the transfer of liquid H_2 in the stationary vertical storage.

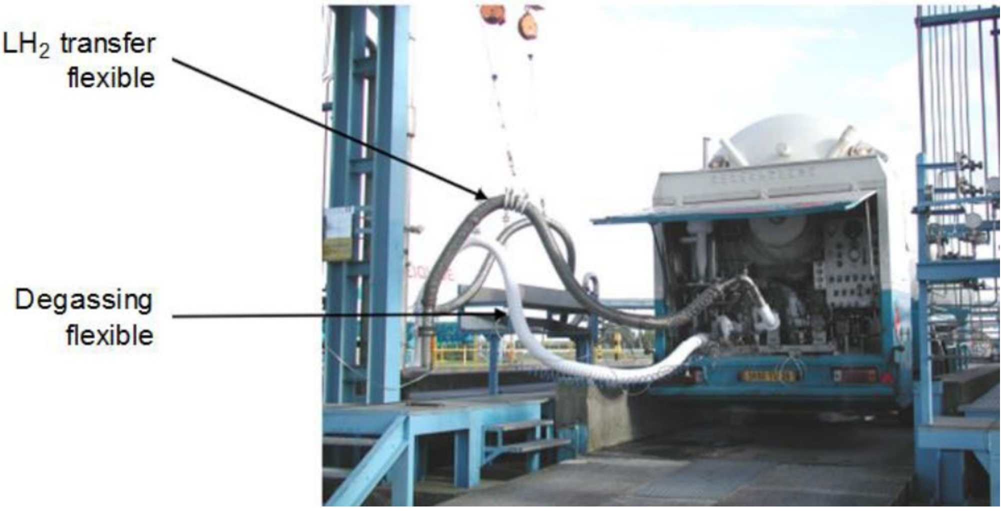

Figure 32. LH_2 transfer line from LH_2 trailer.

In a research and development project called icefuel, with the industry lead partners Evonik and LEONI, a flexible plastic pipe for combined transport of LH_2 and electricity via high temperature superconductor was tested (Figure 33). For insulation, super insulating material and a liquid nitrogen shield was used. The flexible pipeline could be used to supply residential area with chemical and electrical energy and information with an outer diameter of 40 mm only. Maximum transport capacity is 100–200 kW (LHV) [71].

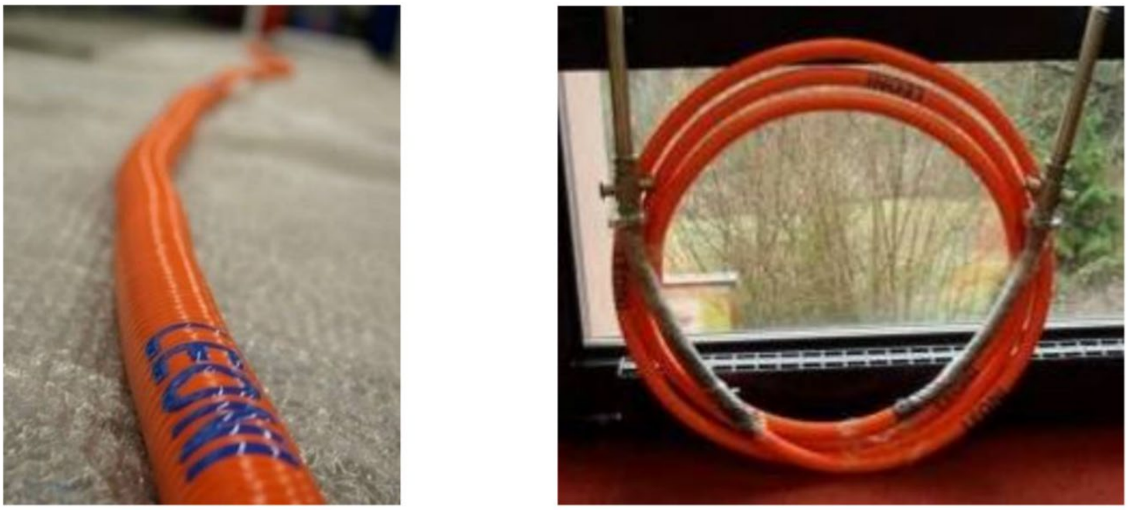

Figure 34. icefuel cable (Courtesy LEONI, Nuremberg).

7.2.4.3 Ship transport

Barges carrying liquid hydrogen have been used for fuel supply within the US and French space programs. Storage containers with a capacity of 947 m^3 of LH_2 (Figure 34) are being used on the way from Louisiana to Florida since the NASA Apollo project, today serving the space shuttle. The European Ariane project was supplied with LH_2 by maritime transportation from New Orleans to Kourou, French Guiana, in 20 m^3 storage vessels with vapor or LN_2 cooled multilayer insulation [72]. These transports were discontinued with the operation of the 5 t/d capacity, on-site liquefaction plant since 1990.

Figure 34. NASA liquid hydrogen barge fleet. (Sources: NASA)

As an important project in the development of a "CO_2-Free Hydrogen Supply Chain", HySTRA, Kawasaki Heavy Industries (KHI) is planning the demonstration of all necessary technologies on a 2017 pilot scale, and the examination of optimized locations, scales, configurations and cost efficiencies of the single chain components [73]. These include:

- hydrogen production in Australia through both brown coal gasification and electrolysis with an overall capacity of 2660 t/yr;
- hydrogen liquefaction at a rate of 4.2 t/d;
- liquid hydrogen carrier ship with cargo capacity of 2500 m^3 for maritime transportation of 873 t/yr from Australia to Japan (corresponding to five roundtrips per year);
- liquid hydrogen stationary storage facility for 3400 m^3;
- hydrogen gas turbine power generation plant with a fuel consumption of 4.2 t/d.

An essential milestone of the HySTRA project was recently achieved with the construction, and completion of the world's first LH_2 carrier ship SUISO FRONTIER launched in December 2019 in Kobe, Japan (Figure 35). The ship has an overall length of 116 m, a width of 19 m, a tonnage of 8000 t and is equipped with a diesel-electric propulsion system reaching a speed of

13.0 kn (~24 km/h) [74]. The cargo ship has currently installed a single LH_2 tank with a capacity of 1250 m^3 featuring a double-shell structure with vacuum insulation in between [75].

Figure 35. SUISO FRONTIER, the world's first LH_2 carrier ship launched in 2019 with LH_2 storage tank [75].

Another major milestone was reached with the completion of an LH_2 receiving terminal in Kobe (Fig. 2-13), also a world's first-of-its-kind, designed to discharge a 2500 m^3-LH_2 cargo. The terminal includes a 2500 m^3 capacity stationary spherical LH_2 tank for longer-term storage [76].

The terminal was built for the CO_2-free Hydrogen Energy Supply-chain Technology Research Association (HySTRA). The Hydrogen Energy Supply Chain (HESC) is a joint Japanese-Australian venture.

Figure 36. KHI LH_2 receiving terminal in Kobe [76].

Commercial scale would need to develop much larger vessels, similar to today's LNG carrier ships of 160,000 m^3 and higher capacity. Various ship designs have been developed within the Euro-Quebec project for future maritime transportation (between Canada and Europe) [77, 78]. The barge carrier considered in the first stage was designed as a dock ship with a total length of 180 m and a width of 29 m carrying five barges (see also previous chapter) to contain a total of 15,000 m^3 of LH_2. Follow-on LH_2 tank ships are the dock ship and the so-called SWATH ship (Small Waterplane Area Twin Hull) developed by the German companies Howaldtswerke Deutsche Werft, Noell-LGA Gastechnik, and Germanischer Lloyd [78]. Both were designed for a load capacity of 125,000 m^3 to take up 8150 tons of LH_2. With a length of more than 300 m, the SWATH ship carries four spherical LH_2 tanks. The hydrogen propulsion system proposed, for which the LH_2 as well as the boil-off losses (~0.1 %/d) is to be used, is a gas turbine with steam injection of 41 MW.

7.2.4.4 Rail transport

The transportation of cryogens in railway tank cars started in the beginning of the 1940s, where LOX was increasingly needed for the steel production. Liquid hydrogen transports in rail cars began in the 1960s by the Linde company using a 107 m^3 tank. The annular space between the inner and outer tanks has a vacuum drawn and is equipped with an insulation system using granular perlite or an alternating wrap of multiple layers of aluminium foil and paper. Measured boil-off rate was 0.2%/d. The US company Praxair is operating a fleet of 16 hydrogen rail cars. They are operated at a working overpressure of 55 kPa with a pressure control system to open the safety relief valve at an overpressure of 117 kPa. The quantities of LH_2 transported in rail cars over long distances (> 1000 km) are about 70 tons [79].

An extensive railway system exists at Baikonur where the cryogenics are moved from the storage tanks to the launch pad by rail cars.

Figure 37 depicts the design of a rail car for liquid hydrogen (and other cryogenic commodities) transports manufactured by the Chinese company CRRC Xi'an Co.,Ltd., a traditional enterprise in railway transportation equipment. The thermally insulated tank with a total volume of 85 m^3 to carry a payload of 5 t can be used for direct loading, unloading, or transfer filling [80].

Figure 37. T85-type liquid hydrogen tank rail car [80].

7.3 Liquid hydrogen refuelling station

Basically, as shown in Figure 38, a LH_2-based refueling station consists of:

- a LH_2 tank (around 20 m^3 - 1000 kg-H_2) with a maximal operating pressure of 10.3 bar,
- an insulated process line from the bottom of the storage to the LH_2 pump, driving LH_2 from the storage tank to a vaporizer; this device allows to pump LH_2 up to 1000 bar,
- a heater (named VAP: hot oil, electric in order to heat up hydrogen at 1000 bar),
- 1000 bar gaseous buffers (few m^3); these buffers are generally bundles of type I or II (i.e. metallic cylinders or long metallic tube).

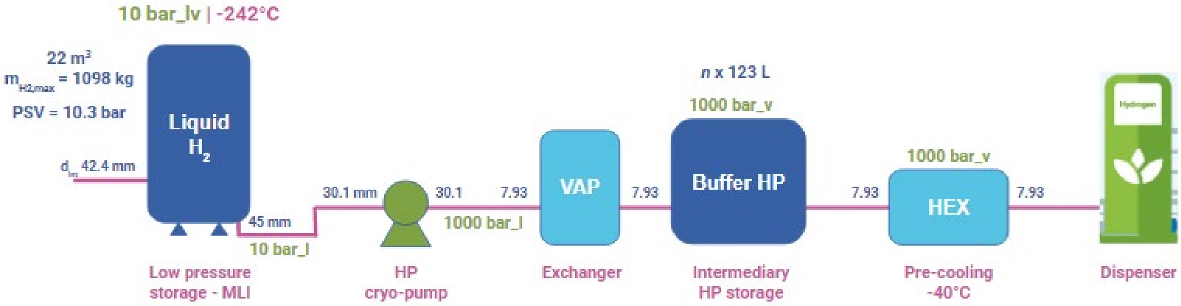

Figure 38. Simplified sketch of a liquid hydrogen refuelling station.

All the other parts (e. g. dispenser, filling hose et al.) of the refueling station are similar to classical gaseous refueling station (see comparison in Figure 39).

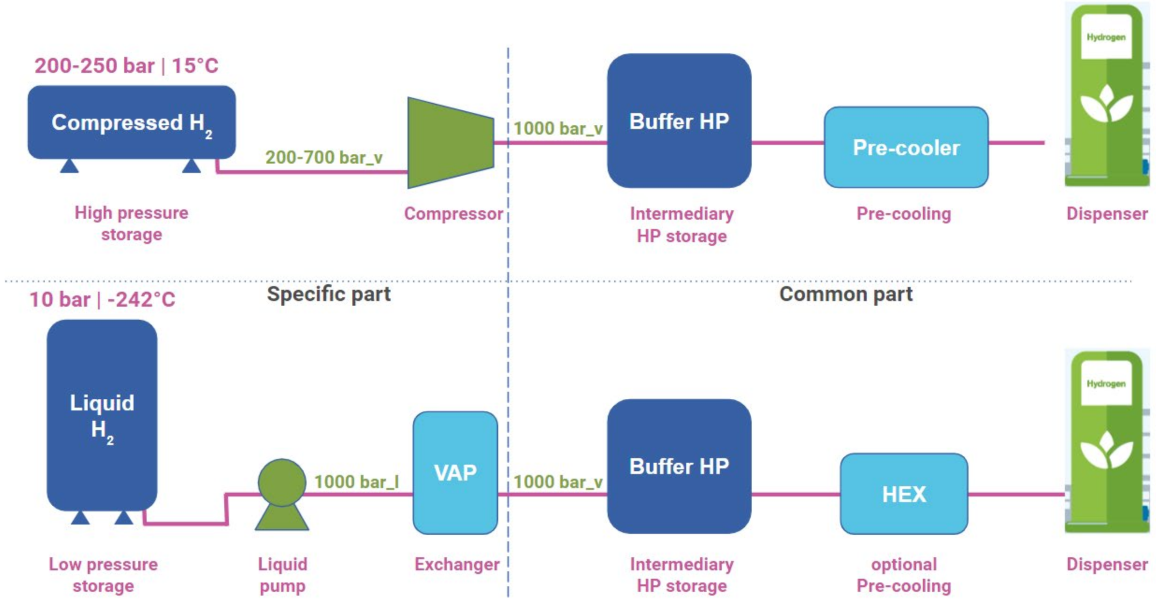

Figure 39. Simplified comparison between gaseous and liquid hydrogen refuelling stations. Top: gaseous HRS, bottom liquid HRS.

The LH_2 tank is delivered by a LH_2 truck. This LH_2 truck is composed of a 40 m^3 horizontal tank operating between 1 and 12 bar (inventory: 4 t-H_2). The connection between the storage and the truck is done by a flexible transfer line. The transfer is performed without a pump. A small vaporizer is present on the trailer to produce a pressure build-up in the truck tank and allow the transfer of liquid hydrogen in the stationary vertical storage.

More concretely below the Linde Liquid hydrogen refuelling station installed at Oakland (US) (see Figure 40).

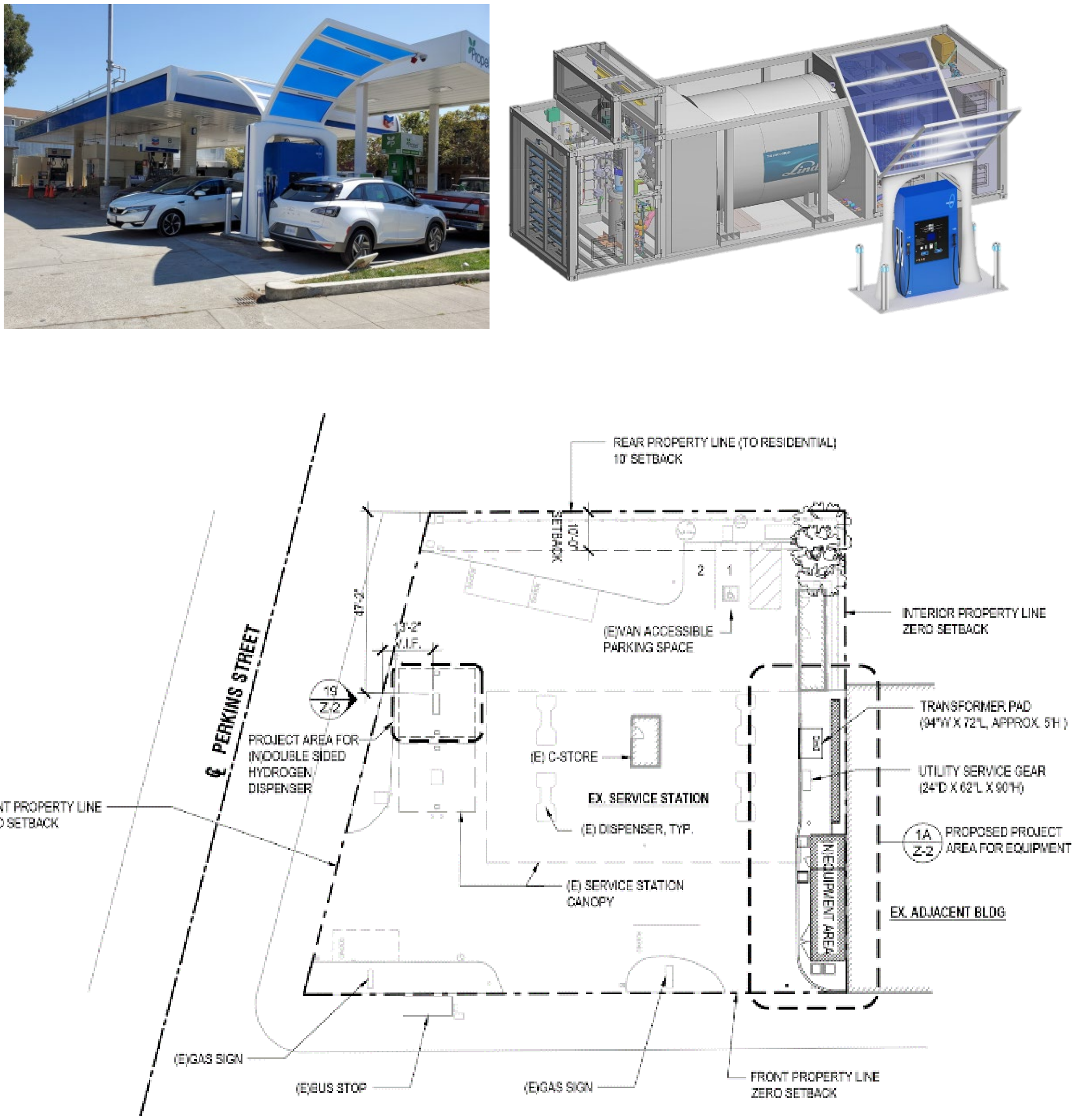

Figure 40. Linde LHRS and layout in Oakland. (Sources: Linde)

Generic process safety features are illustrated and summarized in Figure 41 below.

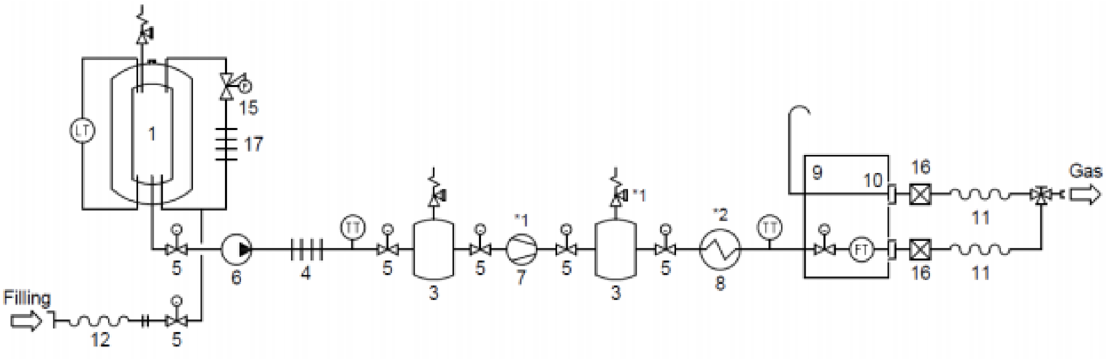

- 1. liquid hydrogen storage unit
- 2. gaseous hydrogen storage unit
- 3. intermediate gas storage
- 4. evaporator
- 5. emergency shutdown system
- 6. pump
- 7. compressor
- 8. chiller
- 9. dispenser
- 10. safety valve
- 11. delivery hose
- 12. off-loading hose
- 13. fill
- 14. purifier
- 15. pressure regulator
- 16. breakaway coupling
- 17. pressure build-up evaporator

- LT level sensor
- FT flow sensor
- TT temperature sensor

Figure 41. Process flow of a LH_2-based refuelling station.

In France, a safety distance of 20 m between public domain and liquid hydrogen source is required. Safety features on liquid refuelling stations are almost the same as for a gaseous refuelling station (see Table 6).

Table 6. Safety features for gaseous/liquid HRS.

What	Where	For what
Qualified and validated hose and fittings	Process and dispenser	Avoid accidental leakages
Periodic replacement of the hose	Dispenser	Avoid accidental leakages
H_2 detection	Inside the process container Inside the dispenser	Activate warning, and shut-off valves if required in case of accidental leakage
Flame (UV/IR) detector	In the process container Outside, close to the dispenser	Activate warning, and shut-off valves if required in case of accidental ignited release
Automatic shut-off valve	Several between H_2 storage and dispenser	Limit H_2 inventory in case of accidental release
Process pressure monitoring	General	Detect abnormal pressure drop due to leak or piping rupture
Naturally ventilated confined spaces	Process container Dispenser	Avoid to reach flammable limits of H_2-air mixture in case of accidental release
Forced ventilation	Process container for some models	Avoid to reach flammable limits of H_2-air mixture in case of accidental release if natural

		ventilation not possible or not efficient enough
ATEX certified equipment	In confined spaces where leaks can occur (i.e. skids and dispenser)	Avoid ignition sources
Hose grounded	Dispenser	Prevent sparks caused by static electricity during refuelling
Automatic leak test before filling	General	Avoid accidental leakages
Flow restrictors	General	Limit flowrate in case of release or piping rupture
Automatic closing time	General	Close H_2 feeding valves in case of hose rupture or leak
Hose break-away device	Dispenser	Avoid major leak by closing feeding flexible in case of tearing by forgetting to disconnect the vehicle
Shock protection (bollard)	Dispenser	Protect the dispenser from major mechanical aggression by vehicle accidental stamping and avoid catastrophic leak
Emergency punch stop	Few meters from the dispenser	Close H_2 feeding valves in case of emergency
Conductive (grounded) concrete slab	Dispenser	Prevent sparks caused by static electricity during refuelling

Table 7 makes a brief overview of available information regarding regulation for liquid hydrogen refuelling stations.

Table 7. Overview of regulation for liquid hydrogen refuelling stations.

Country	Status	Distance to property lines
USA	Permit given by Fire Marshals NFPA55 “recommended”	Lot lines ⇒ 15 m Buildings ⇒ 23 m
France	Storage > 1 t (Europe 5 t) ⇒ authorization given by Prefecture	LH_2 ⇒ 20 m Dispenser (60-120 $g.s^{-1}$) ⇒ 10 m
Germany	No specific regulation for LH_2 if < 5 t (Low Seveso)	LH_2 ⇒ 5 m Dispenser ⇒ 2 m
Japan	Specific LH_2 regulation	LH_2 ⇒ 10 m Dispenser ⇒ 8 m
China	Strictly restricted to military use up to 2018	Under-development

Considering the regulation, it clearly appears a lack of harmonization between the countries both on processes and measures (e.g. authorization required, just recommendations or no specifications; not the same safety distances when defined et al.).

7.4 Liquid hydrogen systems for mobility

7.4.1 Cars

The German car company BMW started as early as 1978 its research on hydrogen-driven cars with a prototype internal combustion engine (ICE). There had been liquid hydrogen storage solutions demonstrated by BMW including safety testing under accidental conditions. Latest H_2 car generation is the BMW Hydrogen 7 (basis: BMW 760iL) of 2006, the first H_2 driven car for which series development process has been applied (Figure 42).

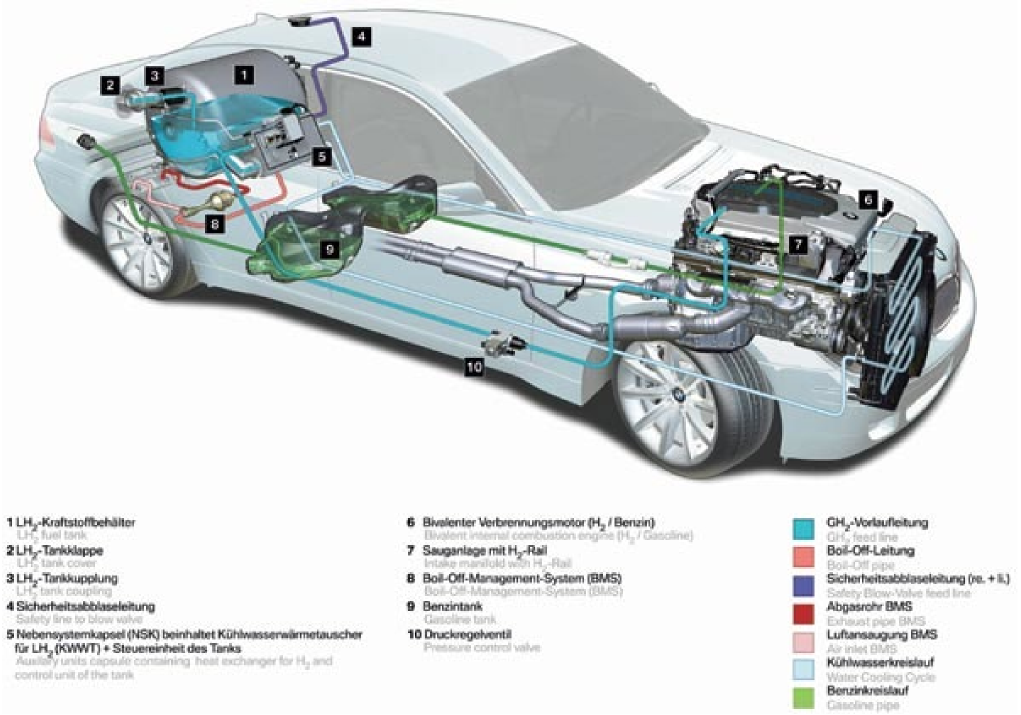

Figure 42. BMW 7 series with LH_2 storage tank and dual fuel (H_2 and gasoline) internal combustion engine (Courtesy of BMW CleanEnergy).

The BMW Hydrogen 7 is equipped with an 8 kg LH_2 tank for a cruising range of about 200 km and an average H_2 fuel consumption of 3.6 kg per 100 km. Although offering certain advantages with the low pressure and high densities the boil-off represents a considerable problem.

Present fuel storage concepts for hydrogen-driven vehicles include both the high-pressure gaseous storage and the cryogenic liquid storage, which requires an appropriate infrastructure including refuelling devices for both modes. In 2004, GH_2 and LH_2 dispensers have been fully integrated into a conventional service station in Berlin (Figure 43) utilized by 17 H_2 driven vehicles (as of May 2007), but with a total capacity of 100 vehicles per day. While the gaseous H_2 is generated on-site by electrolysis, the liquid H_2 is delivered by tank truck. This H_2 filling station is operated by the CEP, a 5-years project of public and private partners to demonstrate production, storage, and distribution of H_2 and the operation, refuelling, and maintenance of H_2 vehicles.

Figure 43. Refueling station for both GH_2 and LH_2 in Berlin (Courtesy BMW Group).

A liquid hydrogen supply system has the advantage of being capable to dispense the H_2 either as liquid or as high-pressure gas avoiding space consuming GH_2 storage. Only one LH_2 storage tank located underground with several tens of tons capacity is employed to serve both modes. Advantages are that separate storage devices for gaseous and liquid H_2 can be avoided as well as separate truck delivery for both modes. Another aim is to reduce filling time. High-pressure gas (70 MPa) is obtained by using newly developed cryogenic pumps which push the liquid into a heat exchanger where it heats up to ambient temperature. This key component is more compact, less noisy and needs less maintenance than a compressor which would be necessary in the case of gas delivery.

The first public station to offer liquid and gaseous hydrogen was opened in 1999 at the airport Munich in Germany and operated until 2006 (when the “ARGEMUC” project was terminated). The LH_2 delivered by truck was filled into a 12 m^3 storage vessel. Refuelling of the vehicle was done automatically by a robot system. In the first two years, ~ 49 m^3 of LH_2 in more than 4000 refuelling processes have been transferred into vehicle tanks. A new public filling station for LH_2 was opened in Munich in 2007 with the storage tank located underground. This station is one of the three mainly dedicated to the BMW Hydrogen 7 fleet.

“Weakest link” in the transfer lines between car tank and dispenser, i.e., the location with the maximum H_2 loss, is the cryogenic coupling. As the tank, it must have a double wall and vacuum insulation. Special constructions are necessary to transfer the cryogenic fuel and making sure that air ingress is avoided. Today’s couplings are working with a floodgate which is purged and purified with helium to remove all air before the valves on either end open at the same time. The refuelling is made through an insulated pipe (“cold finger”) inside the dispenser, which is pushed pneumatically into the filling line of the tank. The gaseous H_2 is removed from the tank and could be – as is the case in the Berlin filling station – routed to a fuel cell plant for electricity generation.

In principle, the problem related to the boil-off might be mitigated with a cryo-compressed storage, typically operated at 50 K and 35 MPa nominally. Such a system might be filled with cryo-compressed hydrogen, LH_2, or with compressed 35 MPa and represents a quite versatile solution.

Solid storage solutions, in particular conventional metal hydrides (Fe and Ti based storage material), are considered to be too heavy for light duty and cars. Although the light metal hydrides come close to the 7% weight performance (mass hydrogen / mass storage system) they require complex thermodynamic management for heat generated during refilling and required for extracting hydrogen.

7.4.2 Buses

Most buses carry the hydrogen as compressed gas. There are, however, a few examples where the hydrogen was stored in liquid form. From the three city buses tested within the Euro-Quebec project in the period 1995–1997, two were based on ICEs using LH_2 as fuel. One was a MAN bus with three super insulated elliptical cryo-tanks with 200 ℓ geometrical volume each to contain a total of 570 ℓ of LH_2 in an underfloor arrangement allowing a cruising range of 250 km (Figure 44). Starting 1996 the bus was test-operated over two years at the airport Munich and in Erlangen, Germany, since 1996. The other bus was of the Van Hool type equipped with two 200 ℓ roof-top-mounted LH_2 tanks as fuel supply system. As part of the EU project EUREKA, a hydrogen bus demonstrator was operated since 1995 using a 700 ℓ LH_2 tank in the rear of the bus to operate a 78 kW fuel cell power system for a 200 km cruising range.

Figure 44. MAN hydrogen-driven fuel cell bus of 1996 with LH_2 storage tanks

7.4.3 Trucks

The Musashi Institute of Technology as part of the Tokyo City University has already a long history (since 1970) in the development and testing of hydrogen-fuelled vehicles with internal combustion engine. Shown in Figure 45 is the 9th generation from 1996, Musashi-9, an LH_2 refrigerator truck where the cold hydrogen is also used to keep the cargo cool [81].

The world's first hydrogen-driven truck was Musashi-7, a modified medium duty truck, presented in 1986. The truck was equipped with a hydrogen-powered engine and with a 150 ℓ LH_2 tank. A high pressure LH_2 pump would provide the fuel to the engine. The pump delivered 8 MPa high pressure hydrogen gas to the engine and the fuel was injected to a hot surface igniter in DI combustion chamber [82].

Figure 45. Musashi-9 LH_2 truck Musashi Institute of Technology [81].

For storage of up to 100 kg of hydrogen currently compressed gaseous hydrogen at 35 to 70 MPa, cryo-compressed hydrogen and liquid hydrogen are investigated. The reference solution is the gaseous form with a 35 MPa Type 4 vessel which are typically integrated behind the driver cabin or above the rear axis. The LH_2 cryostats might be positioned at the same locations where the conventional fuel Diesel is stored. Two cryostats, each with about 500 ℓ empty volume have to be installed. For energy conversion either PEM fuel cells or an H_2 ICE might be chosen depending on the actual application and further criteria. In principle the technologies may be easily derived from the bus application, where more experience is available.

In June 2017 the Zurich engineering company ESORO received the road approval for the world's first fuel cell heavy-duty vehicle. It developed and built a fuel cell truck in the 35-tonne category. On-board storage of high-pressure hydrogen gas is made with seven tanks on a rack with a capacity of totally 34.5 kg of hydrogen [83].

Daimler Trucks announced in 2020 the development of a fuel cell truck, GenH2 (Figure 46), using on board storage of liquid hydrogen. The GenH2 Truck is designed to operate two fuel stacks each comprising 200 cells, for a total power output of 300 kW. Cruising ranges are expected to be in the order of 1000 km on a single tank filling. In cooperation with Linde, the next generation refuelling technology will be developed based on subcooled liquid hydrogen (sLH_2). Daimler Truck AG plans to begin customer trials of the GenH2 Truck in 2023; series production may start in the second half of the decade.

Figure 46. Mercedes FC truck GenH2 concept with LH_2 storage.

7.4.4 Ships

Following an idea of 2014 to substantially reduce pollution in the San Francisco Bay by replacing the diesel-driven ferries with CO_2 emission free, hydrogen-fuelled ships, the Sandia National Laboratory conducted a study on the feasibility of a zero-emission, hydrogen fuel cell, high-speed passenger ferry, called the SF-BREEZE [84]. The ship is designed as a commuter ferry for 150 passengers to travel four 50 nm (~93 km) round-trip routes each day at a top speed of 35 knots (~65 km/h). Figure 47 shows a schematic of SF-BREEZE [84]. The on-board storage of fuel was selected to be liquid hydrogen to minimize the weight and thus enhance the ship's performance. A total of 1200 kg (or 17 m^3) of LH_2 are stored in a single tank installed on the roof. Power is provided by 41 PEMFC racks, each rack composed of four 30 kW FC stacks amounting to a total of 4.92 MW.

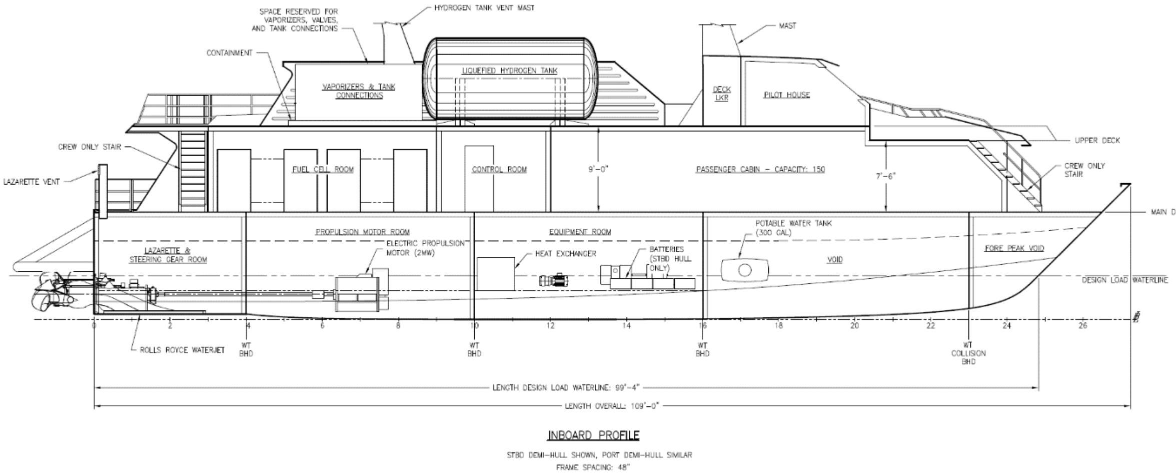

Figure 47. SF-BREEZE hydrogen fuel cell based high speed passenger ferry [86].

The Norway-based shipping company Norled has started the development of hydrogen-powered car ferries considering two options for the storage of the hydrogen fuel, as liquid or as compressed gas (Figure 48). For the cryo-version, Linde will supply both the liquid hydrogen and the related infrastructure. Power is provided by two 200-kW fuel cell modules. The LH_2 tank will be installed on the roof [85].

Figure 48. On-deck arrangement of LH_2 storage, fuel cell and vent mast on the NORLED ferry [85].

Starting in 2021 the EU project HySHIP with 14 partners and led by the Norwegian shipping operator Wilhelmsen targets at the development of a zero-emission prototype ship with hydrogen propulsion. It is based on the so-called 'Topeka" concept (Figure 49) planned to operate between the offshore supply bases on the Norwegian west coast. The ship will be equipped with a 3 MW PEM fuel cell stack and supported by a 1 MWh battery pack for the purpose of optimization of load and efficiency of the fuel cells. On-board storage of hydrogen will be a single LH_2 tank installed on the roof.

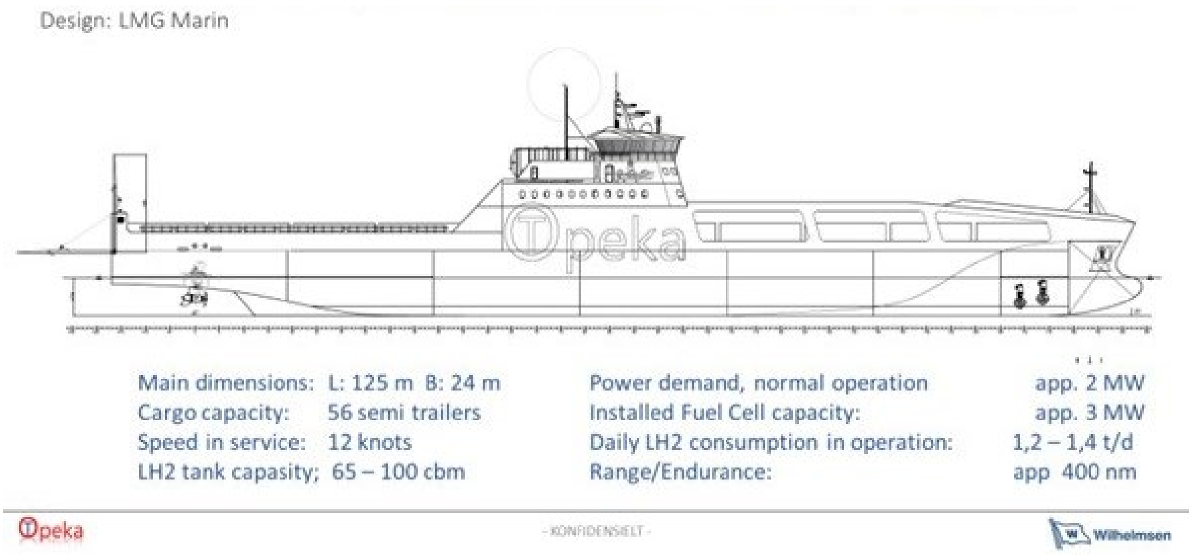

Figure 49. Design of the TOPEKA prototype FC ship with on-board storage of LH_2 [86].

7.4.5 Aircrafts

The idea to use LH_2 as aircraft fuel was considered since the early 20th century stressing that H_2 had a greater heat content than any other fuel, higher fuel flight efficiency, lighter weight, less noise, and reduced pollution. In terms of safety, LH_2 is expected to be safer than the conventional kerosene due to smaller endangered areas and shorter fire duration.

The first successful in-flight test of an experimental hydrogen-propelled aircraft was made in the USA. In a B-57B twin-engine aircraft, one turbojet engine was converted to run on both JP-4 and hydrogen fuel (Figure 50). The stainless-steel tank for the LH_2 on the left-wing tip was 6.2 m long, had a volume of 1.7 m^3 and a 50 mm plastic foam insulation. The aircraft was supposed to start with the conventional JP-4 fuel, be switched to H_2 fuel at an altitude of ~ 16,400 m, before switched back to JP-4 and return to the ground under normal operational conditions [87]. Due to the significant loss of LH_2 fuel during chill-down of all LH_2 lines, it was considered wise to have the chill-down process made with liquid helium on ground prior to the flight [88]. On Feb. 13, 1957, the first of three successful flights took place. The one engine operated on H_2 for about 20 min at a speed of Mach 0.72 before the fuel tank was running empty [87].

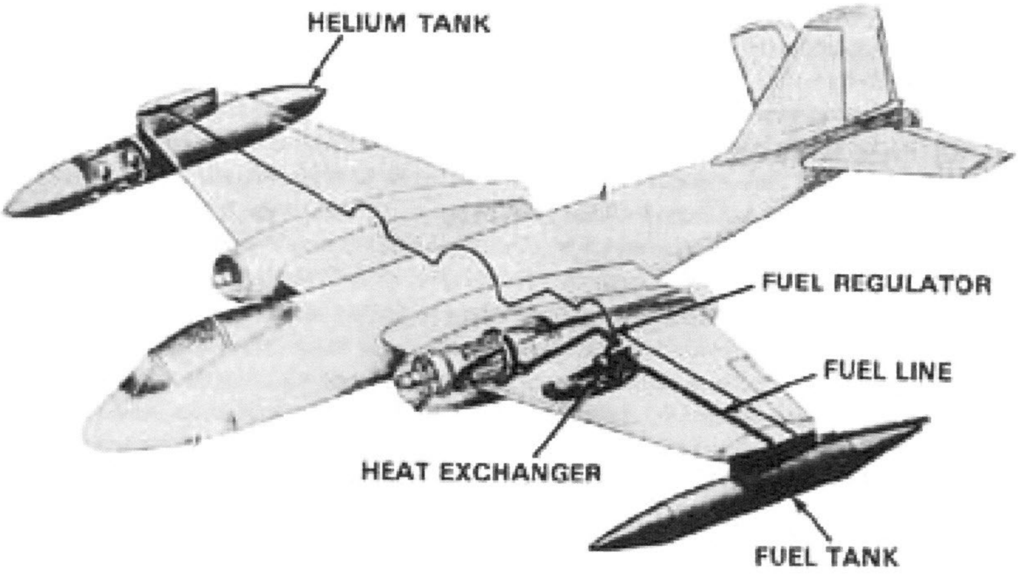

Figure 50. B-57B twin-engine aircraft with one engine fuelled by LH_2 successfully operated first in 1956 [87].

In 1988, a four-seater Grumman Cheetah with an LH_2 fueled internal combustion engine became the first and sole, so far, airplane to take off, cruise, and land by means of hydrogen power only [89], although it was a 36 s flight only.

In the same year, the Russian company ANTK-Tupolev has operated the "Flying Laboratory" Tu-155 (Figure 51), which is a hybrid version of the Tu-154 airplane [90]. One of the three engines ("NK-88"), the one in central position, could be fuelled with either hydrogen or natural gas stored in a 17.5 m^3 capacity tank. The maiden flight on April 15, 1988, lasted 21 min; total operating experience with LH_2 accumulated to 10 hours [91].

Figure 51. Tupolev 155 “Flying Laboratory” of 1988 with the central engine fuelled by LH_2 or LNG [91].

Recently, Airbus unveiled three concepts for a hydrogen-fuelled “ZEROe” aircraft that utilize liquid hydrogen to power modified gas turbine engines. Shown in Figure 52 is the turboprop concept for short-range flights and a cruising range of more than 1000 nautical miles (~1852 km).

Figure 52. One design of the Zero Emission Airbus [92].

On 21st September 2020, Airbus has revealed three concepts (turbofan design, turboprop design and ‘blended-wing body’ design) for the world’s first zero-emission commercial aircraft which could enter service by 2035. These concepts each represent a different approach to achieving zero-emission flight, exploring various technology pathways and aerodynamic configurations in order to support the company's ambition of leading the way in the decarbonisation of the entire aviation industry. (see Figure 53).

All of these concepts rely on hydrogen as a primary power source. In the turbofan and turboprop configurations, two hybrid hydrogen turbofan engines provide thrust. The liquid hydrogen storage and distribution system is located behind the rear pressure bulkhead. This is an option which Airbus believes holds exceptional promise as a clean aviation fuel and is likely to be a solution for aerospace and many other industries to meet their climate-neutral targets.

Figure 53 Airbus ZEROe concept aircrafts. Turbofan, 'blended-wing body' and turboprop designs from up down.

8. Liquid hydrogen hazards and associated risk for Responders

Health hazards associated with the release of liquid hydrogen are outlined below.

- Contact with liquid hydrogen or its splashes on the skin or in the eyes can cause serious cold burns by *frostbite or hypothermia.*
- *Cryogenic burns* can also result from contact of unprotected parts of human body with either cold fluids or cold surfaces.
- Inhalation of cold hydrogen vapours may cause *respiratory discomfort* and can result in *asphyxiation*.
- Direct physical contact with LH_2, cold vapours or cold equipment can cause serious *tissue damage.* Momentary contact with a small amount of the liquid may not pose as great a

danger of a burn because a protective film of evaporating gaseous hydrogen may form. Danger of freezing occurs when large amounts are spilled, and exposure is extensive[2].

- Personnel should not touch cold metal parts and they should wear *protective clothing*. They also need to protect the affected area with a loose cover.
- *Cardiac malfunctions* are likely when the internal body temperature drops to 27°C or lower, and death may result when the internal body temperature drops lower than 15°C.
- *Asphyxiation* is also possible if liquid hydrogen released and vaporised indoors.

Friedrich et al. [42] measured sound levels from unignited and ignited cryogenic jets (nozzle diameter 1 mm, pressure up to 30 bar, hydrogen mass flow rate up to 8 g/s, temperature 34 - 65 K). Please note that the sound level will depend on the spouting pressure and the mass flow rate. Four different meters for sound level evaluation were installed at distances of 1.23 m, 1.65 m, 2.91 m, and 4.55 m to the release nozzle inside a testing cell [42]. The steady-state levels of the sound meter signals are illustrated in Figure 54. 'The ignited jets generated about 10 dB (A) higher sound levels compared to unignited jets. There seems to be a weak increase of the sound level with increasing hydrogen mass flow rate. The initial burn-out of the hydrogen inventory in the unreacted jet causes the highest sound emissions' [42].

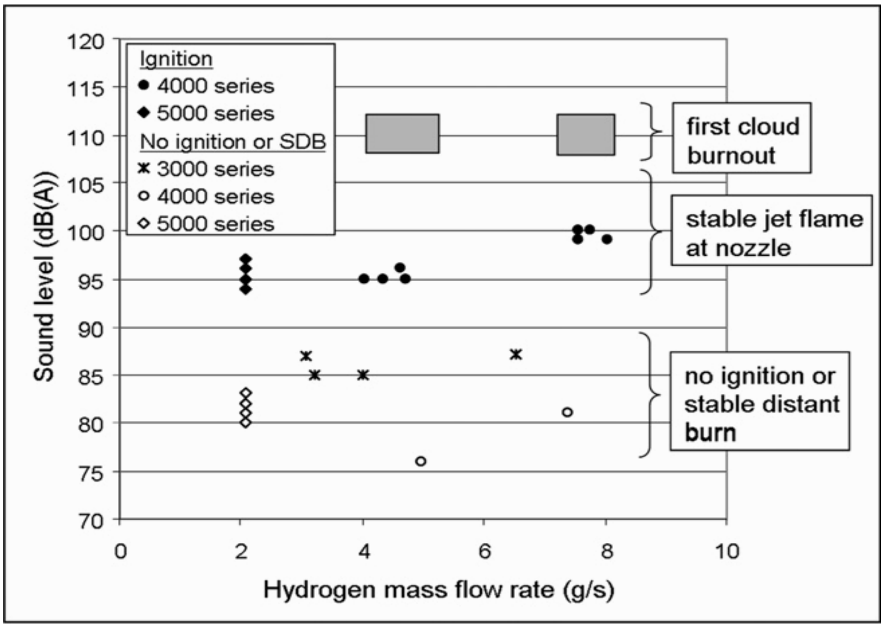

Figure 54. Measured sound levels from ignited and unignited stationary cryogenic hydrogen jets [42]

The sound levels measured in this study (≤112 dB(A)) are considered hazardous only in case of permanent or long-time exposures. An ear damage from short sound waves becomes possible for 120 dB(A) and above. 'So the sound levels from unignited and ignited cryogenic hydrogen jets measured in this study pose no health hazards, even at the close distances

---

[2] Effect of liquid nitrogen: https://www.youtube.com/watch?v=F9dhZJQk80A&feature=youtu.be&t=291

investigated (1.2 - 4.5 m). On the other side, the measured sound levels are loud enough to allow an early identification and location of a free hydrogen jet or jet flame with sound meters' [42].

Regarding safety properties of liquid hydrogen and behaviour after release, it appears that - in order to well manage the risk of the existing applications and potential future applications - it is necessary to take into account knowledge developed for gaseous hydrogen hazard as well. At present time, considering hydrogen energy activities and applications, liquid hydrogen is mainly used for storing higher amounts of hydrogen. Thus, the main liquid hydrogen systems are the liquid trailers for hydrogen delivery and liquid hydrogen storages. Systems with on-board liquid hydrogen are not largely deployed, but several on-going projects studied future liquid hydrogen-based fuel cell transportation means like ships, trains and planes.

9. Safety measures and engineering solutions

Hydrogen transportation and distribution pose specific issues in terms of safety. The issues are strongly related to the chemical and physical properties of hydrogen: its ability to embrittle materials, its ease in escaping from containment, its wide flammability range, and the limited amount of energy needed to ignite it, all represent barriers to safe use. At the same time, its extremely low density is a guarantee that the gas will likely ascend instead of forming dense dangerous clouds as other hazardous gases do.

A major problem when producing and handling liquid hydrogen is the potential contamination of the hydrogen with air or other impurities which will, with the exception of helium, freeze and might block then pipes, filters or armatures.

On the exterior of poorly insulated containers or pipes the cryogenic temperatures may condense air with serious enrichment of oxygen. Liquid or frozen solid oxygen promotes ignition and oxidizes easily materials which are usually non-flammable.

The extreme low temperatures require careful selection of materials. Conventional carbon steels will suffer from a transition to nil ductility (NDTT). Aluminium or stainless steels are typically suitable structural materials for cryogenic hydrogen and welded connections are preferred to screwed connections. If, however, cryogenic hydrogen is leaking, it might lead also to condensation of air and to hazardous oxygen enrichment. The leaking cryogenic hydrogen is as heavy as ambient air. This suppresses buoyancy effects and promotes dispersion of flammable mixtures on ground level.

Countermeasures are careful purity control of the feed hydrogen and purging the cold boxes with helium. Leaks may be detected by temperature drop and visually identified via the fog formed from condensation of ambient humidity.

Safety considerations are related to the separation of the LH_2 containing facilities from roads, buildings, or runways, the ventilation for enclosed areas, the preclusion of air ingress, automated system shutdowns, confinement and control of large-scale spills, or the use of nonsparking electric devices. Particularly numerous LH_2 refueling processes increase the possibility of a potential accumulation of impurities, solid N_2 or O_2, which enhance the risk of fuel system component damage and explosion. Conventional warm-up in order to vaporize impurities is not practicable for frequently used tanks.

Both kinds of analyses generally start from the definition of an event tree that allows selecting and concentrating on more representative and risky combinations. The possible initiating events are those that might affect natural gas pipelines (e.g. external events, impacts, mechanical or service failures, etc.). The good buoyancy of hydrogen has been taken into account by analysts in order to be accurate in forecasting the behaviour of a gas leakage in the atmosphere and wind direction and speed are here particularly influent. The very wide flammability range does not work in favour of safety but the buoyancy decreases the possibility of cloud formations at low heights (where human receptors are closer). In the event that large clouds are produced, these can be lately ignited and cause explosions. Another possibility is the formation of jet fires due to leakages in pipelines under pressure with an ignition that is not too much delayed. The safety distance for receptors, both humans and buildings, depends on many factors.

As in the usual practice of risk prevention, artificial barriers may be inserted to decrease the safety distances from the possible release point to the receptor. In the case of hydrogen, barriers have been studied and proposed for application and vary in size, height, and inclination. For example, NFPA 55 [93] proposes a 60° inclined barrier to protect from jet fires originating from storages. In Royle and Willoughby [41] these barriers have been tested against vertical ones and showed mixed response, being more suitable to protect the leakage area against overpressure and heat flux but less efficient to protect the area behind the barrier from the heat flux. A vertical barrier proved more efficient at protecting receptors behind it.

It should be noted that the contents of this lecture are extracted from the deliverable D6.1 “Handbook of hydrogen safety: Chapter on LH_2 safety” [94]. Within the PRESLHY project an entire deliverable D6.2 “Guidelines for safe design and operation of LH_2 infrastructure” has been dedicated to the aspects of LH_2 safety.

References

1. Rossini FD. A report on the international practical temperature scale of 1968. Commission I.2: Thermodynamics and thermochemistry. International union of pure and applied chemistry. P.557-P.570.
2. Cengel, Yunus A. and Turner, Robert H. (2004). Fundamentals of thermal-fluid sciences, McGraw-Hill, p.78.
3. Klier J., et al, A new cryogenic high-pressure H_2 test area: First results. Proc 12th IIR Int Conf, Dresden (2012).

4. Edeskuty F.J., Stewart W.F., Safety in the handling of cryogenic fluids. The International Cryogenics Monograph Series, Plenum Press, New York (1996).
5. Bonhoeffer, K.F., Harteck, P. Experimente über Para- und Orthowasserstoff. Naturwissenschaften 17, 182 (1929).
6. Karlsson E., Catalytic ortho- to parahydrogen conversion in liquid hydrogen. (2017). Available at https://www.semanticscholar.org/paper/Catalytic-ortho-to-parahydrogen-conversion-in-Karlsson/d90cd059e742fe7ea68bb86130ce6b770ec496d1 [access on 04.04.2021]
7. Astbury G.R., Hawksworth S.J., Spontaneous ignition of hydrogen leaks: A review of postulated mechanisms. 1st Int Conf Hydrogen Safety (ICHS-1), Pisa (2005).
8. Zabetakis M.G., Safety with cryogenic fluids. Plenum Press, New York (1967).
9. Eichert H., et al. Gefährdungspotential bei einem verstärkten Wasserstoffeinsatz. Study for the Büro für Technikfolgenabschätzung des Deutschen Bundestags, Deutsches Zentrum für Luft- und Raumfahrt (DLR), Stuttgart (1992).
10. Kuznetsov M., Czerniak M., Grune J., Jordan T., Effect of temperature on laminar flame velocity for hydrogen-air mixtures at reduced pressures. Proc. 5th Int Conf Hydrogen Safety (ICHS-5), Brussels (2013), paper 231.
11. Proust C., INERIS research performed within PRESLHY. Presentation at the 13th Int Symp Hazards, Prevention, and Mitigation of Industrial Explosions (ISHPMIE), Braunschweig (2020).
12. NASA. Report of the Presidential Commission on the Space Shuttle Challenger accident (1986). (1997). Available at http://science.ksc.nasa.gov/shuttle/missions/51-l/docs/rogers-commission/table-of-contents.html [access 04.04.2021]
13. Cirrone DMC, Makarov D, Molkov V. Simulation of thermal hazards from hydrogen under-expanded jet fire. International Journal of Hydrogen Energy, 44(17), 2019, pp 8886-8892.
14. Hardee H.C., Lee D.O., Thermal hazard from propane fireballs. Transportation Planning and Technology 2 (1973) 121–128.
15. Zabetakis M.G., Burgess D.S., Research on the hazards associated with the production and handling of liquid hydrogen. Report No. WADD TR 60-141, Wright Air Development Division, OH (1960).
16. Makarov D., Shentsov V., Kuznetsov M., Molkov V., Hydrogen tank rupture in fire in the open atmosphere: Hazard distance defined by fireball. Hydrogen 2(1) (2020) 134–146.
17. Ustolin F., Paltrinieri N., Hydrogen fireball consequence analysis. Chemical Engineering Transactions 82 (2020) 211–216.

18. Ustolin F., Paltrinieri N., Landucci G., An innovative and comprehensive approach for the consequence analysis of liquid hydrogen vessel explosions. J Loss Prevention in the Process Industries 68 (2020) 104323.
19. Pehr K., Aspects of safety and acceptance of LH_2 tank systems in passenger cars. Int J Hydrogen Energy 21(5) (1996) 387–395.
20. Kobayashi H., et al., Experiment of cryo-compressed (90-MPa) hydrogen leakage diffusion. Int J Hydrogen Energy 43(37) (2018) 17928–17937.
21. Molkov V., Makarov V., Bragin M.V., Physics and modelling of underexpanded jets and hydrogen dispersion in atmosphere. Physics of Extreme States of Matter (2009) 146–149.
22. Hecht E.S., Panda P.P., Mixing and warming of cryogenic hydrogen releases. Int J Hydrogen Energy 44(17) (2019) 8960–8970.
23. Simoneau R., Hendricks R., Two-phase choked flow of cryogenic fluids in converging-diverging nozzles. NASA Tech. Rep. Pap. 1484 (1979).
24. Travis J.R., Piccioni Koch D., Breitung W., A homogeneous non-equilibrium two-phase critical flow model. Int J Hydrogen Energy 37(22) (2012) 17373–17379.
25. Venetsanos A.G., Homogeneous non-equilibrium two-phase choked flow modeling. Int J Hydrogen Energy 43(50) (2018) 22715–22726.
26. Leachman J.W., Jacobsen R.T., Penoncello S.G., Lemmon E.W., Fundamental equations of state for parahydrogen, normal hydrogen, and orthohydrogen. J Physical and Chemical Reference Data 38 (2009) 721.
27. Venetsanos A.G., Bartzis J.G., CFD modeling of large-scale LH_2 spills in open environment. Int J Hydrogen Energy 32(13) (2007) 2171–2177.
28. Venetsanos A.G., Giannissi S.G., Release and dispersion modeling of cryogenic under-expanded hydrogen jets. Int J Hydrogen Energy 42(11) (2017) 7672–7682.
29. Friedrich A., et al., Ignition and heat radiation of cryogenic hydrogen jets. Int J Hydrogen Energy 37(22) (2012) 17589–17598.
30. Lachance J., Tchouvelev A., Engebo A., Development of uniform harm criteria for use in quantitative risk analysis of the hydrogen infrastructure. Int J Hydrogen Energy 36(3) (2011) 2381–2388.
31. Panda P.P., Hecht E.S., Ignition and flame characteristics of cryogenic hydrogen releases. Int J Hydrogen Energy 42(1) (2017) 775–785.
32. Saffers J.B., Molkov V.V., Towards hydrogen safety engineering for reacting and non-reacting hydrogen releases. J Loss Prevention in the Process Industries 26(29 (2013) 344–350.

33. Cirrone D., Makarov D., Molkov V., Cryogenic hydrogen jets: Flammable envelope size and hazard distances for jet fire. Proc. 8th Int Conf on Hydrogen Safety (ICHS2019), Adelaide, Australia (2019) paper 191.
34. Cirrone D., Makarov D., Molkov V., Thermal radiation from cryogenic hydrogen jet fires. Int J Hydrogen Energy 44(17) (2019) 8874–8885.
35. Breitung W., et al., Experimental and theoretical investigations of sonic hydrogen discharge and jet flames from small breaks. Final Report for project ICEFUEL, Karlsruhe Institute of Technology (2009).
36. Hankinson G and Lowesmith B J (2012) A consideration of methods of determining the radiative characteristics of jet fires. Combust Flame 159:1165–1177.
37. Ekoto I.W., et al., Updated jet flame radiation modeling with buoyancy corrections. Int J Hydrogen Energy 39(35) (2014) 20570–20577.
38. Molina A., Schefer R.W., Houf W.G., Radiative fraction and optical thickness in large-scale hydrogen-jet fires. Proc Combustion Institute 31(2) (2007) 2565–2572.
39. Takeno K., et al., Dispersion and explosion field tests for 40 MPa pressurized hydrogen. Int J Hydrogen Energy 32 (2007) 2144–2153.
40. Grune J., Sempert K., Kuznetsov M., Jordan T., Experimental study of ignited unsteady hydrogen releases from a high pressure reservoir. Int J Hydrogen Energy 39(11) (2013) 6176–6183.
41. Royle M., Willoughby D.B., Consequences of catastrophic releases of ignited and unignited hydrogen jet releases. Int J Hydrogen Energy 36(3) (2010) 2688–2692.
42. Friedrich, A. et al. (2012). Ignition and heat radiation of cryogenic hydrogen jets. International Journal of Hydrogen Energy. Vol.31, pp.17589-17598.
43. Brennan S., Molkov V., Safety assessment of unignited hydrogen discharge from onboard storage in garages with low levels of natural ventilation. Int J Hydrogen Energy 38(19) (2013) 8159–8166.
44. Brennan S., Molkov V., Pressure peaking phenomenon for indoor hydrogen releases. Int J Hydrogen Energy 43(39) (2018) 18530–18541.
45. Makarov D., Shentsov V., Kuznetsov M., Molkov V., Pressure peaking phenomenon: Model validation against unignited release and jet fire experiments. Int J Hydrogen Energy 43(19) (2018) 9454–9469.
46. Lach A.W., Gaathaug A.V., Vaagsaether K., Pressure peaking phenomena: Unignited hydrogen releases in confined spaces – Large-scale experiments. Int J Hydrogen Energy 45(56) (2020) 32702–32712.

47. Lach A.W., Gaathaug A.V., Large scale experiments and model validation of Pressure Peaking Phenomena-ignited hydrogen releases. Int J Hydrogen Energy 46(11) (2021) 8317– 8328.

48. Hussein H.G., Brennan S., Shentsov V., Makarov D., Molkov V., Numerical validation of pressure peaking from an ignited hydrogen release in a laboratory-scale enclosure and application to a garage scenario. Int J Hydrogen Energy 43(37) (2018) 17954–17968.

49. Brennan S., Hussein H.G., Makarov D., Shentsov V., Molkov V., Pressure effects of an ignited release from onboard storage in a garage with a single vent. Int J Hydrogen Energy 44(17) (2019) 8927–8934.

50. Babrauskas V., Estimating large pool fire burning rates. Fire Technology, 19 (1983) 251-261.

51. Rew P.J., Hulbert W.G., Development of pool fire thermal radiation model. HSE Contractor Report WSA/RSU8000/018, UK (1995).

52. Luketa-Hanlin A., A review of large-scale LNG spills: Experiments and modeling. J Hazardous Materials 132(2–3) (2006) 119–140.

53. Hall J.E., Hooker P., Willoughby D. Ignited releases of liquid hydrogen: Safety considerations of thermal and overpressure effects. Int J Hydrogen Energy 39 (2014) 20547–20553.

54. Cassut L.H., et al., A study of the hazards in the storage and handling of liquid hydrogen. Advances in Cryogenic Engineering 5 (1960) 55–61.

55. ADL. Final report on an investigation of hazards associated with the storage and handling of liquid hydrogen. Report C-61092, Arthur D. Little Inc., Cambridge, MA (1960).

56. Zabetakis M.G., et al., Explosion hazards of liquid hydrogen. Advances in Cryogenic Engineering 6 (1961) 185–194.

57. Witcofski R.D., Chirivella J.E., Experimental and analytical analyses of the mechanisms govering the dispersion of flammable clouds formed by liquid hydrogen spills. Int J Hydrogen Energy 9(5) (1984) 425–435.

58. Urano Y., et al. Hazards of burning liquefied hydrogen. Part 1: Flame of stable burning. Part 2: Flame of abnormal burning. National Chemical Laboratory for Industry 81 (1986) 143–157 (In Japanese).

59. Verfondern K., Dienhart B., Experimental and theoretical investigation of liquid hydrogen pool spreading and vaporization. Int J Hydrogen Energy 22(7) (1997) 649–660.

60. Dorofeev S.B., Kuznetsov M.S., Alekseev V.I., Efimenko A.A., Breitung W., Evaluation of limits for effective flame acceleration in hydrogen mixtures. J Loss Prevention in the Process Industries 14(6) (2001) 583–589.

61. Dorofeev S.B., Sidorov V.P., Kuznetsov M.S., Matsukov I.D., Alekseev V.I., Effect of scale on the onset of detonations. Shock Waves 10 (2000) 137–149.

62. Asadnia, Large-scale liquid hydrogen production methods and approaches: A review. Applied Energy 212 (2018) 57–83.

63. Funke T., Development of large scale hydrogen liquefaction. Presentation at the Hydrogen Liquefaction & Storage Symp, Perth (2019).

64. Decker L., Latest global trend in liquid hydrogen production. Presentation at the HYPER Closing Seminar, Brussels (2019).

65. GTR, Proposal for a Global Technical Regulation (GTR) on hydrogen fuelled vehicles, 2013. ECE/TRANS/WP.29/GRSP/2013/41. United Nations. Economic Commission for Europe. Inland Transport Committee. World Forum for Harmonization of Vehicle Regulations, 160th Session, Geneva, 25-28 June 2013.

66. Royle, M and Willoughby, D (2012). Releases of unignited liquid hydrogen. HSL Report XS/11/70. Available from HSL: Buxton.

67. Decker L., Liquid hydrogen distribution technology. Presentation at the HYPER Closing Seminar, Brussels (2019).

68. Krieg D., Konzept und Kosten eines Pipelinesystems zur Versorgung des deutschen Straßenverkehrs mit Wasserstoff. Series Energy&Environment Vol 144, Research Center Jülich (2012).

69. Zittel W., Wurster R., Bölkow L., Hydrogen in the energy sector. TÜV SÜD Industrie Service GmbH (1996). Available at http://www.hyweb.de/Knowledge/w-i-energiew-eng.html}.(BibTeX) [access 04.04.2021]

70. Mei R.W., Klausner J., Project title: Chill down processes of hydrogen transport pipelines. Report NASA/CR-2006-214091, National Aeronautics and Space Administration, Washington DC (2006).

71. Markowz G., Dylla A., Elliger T., icefuel® – An infrastructure system for cryogenic hydrogen storage, distribution and decentral use. Proc 18th World Hydrogen Energy Conference (WHEC-18), Essen, Report Energy & Environment, Vol. 78-1, Research Center Jülich (2010).

72. Peschka W. Liquid hydrogen: Fuel of the future. Springer-Verlag Wien New York (1992).

73. Oyama S., Kamiya S., Harada E., Inoue K., Nishimura M., CO_2-free hydrogen supply chain project and risk assessment for the safety design. Proc. 5th Int Conf on Hydrogen Safety (ICHS-5), Hamburg (2013) paper 171.

74. KHI, World's first liquefied hydrogen carrier SUISO FRONTIER launches building an international hydrogen energy supply chain aimed at carbon-free society (2019). Available

at https://global.kawasaki.com/en/corp/newsroom/news/detail/?f=20191211_3487 [access on 04.04.2021]

75. KHI, Kawasaki completes installation of liquefied hydrogen storage tank for marine transport applications on world's first liquefied hydrogen carrier. (2020). Available at https://global.kawasaki.com/en/corp/newsroom/news/detail/?f=20200309_3090 [access on 04.04.2021]
76. KHI, Kawasaki completes world's first liquefied hydrogen receiving terminal Kobe LH_2 terminal (Hytouch Kobe). (2020). Available at https://global.kawasaki.com/en/corp/newsroom/news/detail/?f=20201203_2378 [access on 04.04.2021]
77. Giacomazzi G., Gretz G., Euro-Quebec Hydro-Hydrogen Project (EQHHPP): A challenge to cryogenic technology. Cryogenics 33 (1993) 767–771.
78. Petersen U., et al., Design and safety considerations for large-scale sea-borne hydrogen transport. Int J Hydrogen Energy 19 (1994) 597–604.
79. Hudders R.S., Dorf C.J., Holcombe A.H., Railway tank car for transcontinental shipment of liquefied hydrogen. In: Timmerhaus K.D. (ed), Advances in Cryogenic Engineering 8 (1963) 461–466.
80. CRRCGC, T85 Type Liquefied Hydrogen Tank Car. (2016). Available at https://www.crrcgc.cc/xaen/g11117/s21282/t271695.aspx [access on 04.04.2021]
81. Yamane K., et al., Some performance of engine and cooling system of LH_2 refrigerator van Musashi-9. Int J Hydrogen Energy 21(9) (1996) 807–811.
82. Takiguchi M., Furuhama S., Suzuki T., Tsujita M., Combustion improvement of liquid hydrogen fueled engine for medium-duty trucks. Proc. 4th Int Pacific Conf Automotive Engineering, Melbourne (1987).
83. FCB, Fuel Cells Bulletin 2016(12) 14–15.
84. Pratt J.W., Klebanoff L.E., Feasibility of the SF-BREEZE: a Zero-Emission, Hydrogen Fuel Cell, High-Speed Passenger Ferry. Report SAND2016-9719, Sandia National Laboratory, Livermore CA (2016).
85. NORLED, World's first ship driven by LH_2. Presentation at GCE Ocean Technology workshop, Floro, Norway (2019). Available at https://www.gceocean.no/media/2683/norled.pdf [access on 04.04.2021].
86. Turner J., HySHIP: inside Europe's flagship hydrogen ship demonstrator project. (2020). Available at https://www.ship-technology.com/features/hydrogen-vessel/ [access on 04.04.2021].
87. Sloop J.L., Liquid hydrogen as a propulsion fuel, 1945-1959. NASA History Office. Report NASA SP-4404. National Aeronautics and Space Administration, Washington DC (1978).

88. Dawson V.P., Bowles M.D., Taming liquid hydrogen: The Centaur upper stage rocket 1958-2002. The NASA History Series, Report NASA SP-2004-4230. National Aeronautics and Space Administration, Washington DC (2004).

89. Peschka W. Liquid hydrogen: Fuel of the future. Springer-Verlag Wien New York (1992).

90. DASA. CRYOPLANE – Deutsch-Russisches Gemeinschaftsprojekt zum Einsatz kryogener Treibstoffe in der zivilen Luftfahrt – Realisierbarkeitsstudie 1990/91/92. Report, Deutsche Aerospace Airbus GmbH, Hamburg (1992).

91. Tupolev. Development of cryogenic fuel aircraft. (2008). Available at http://www.tupolev.ru/English/Show.asp? SectionID=82 [access on 04.04.2021]

92. Airbus, Airbus reveals new zero-emission concept aircraft. (2020). Available at https://www.airbus.com/newsroom/press-releases/en/2020/09/airbus-reveals-new-zeroemission-concept-aircraft.html [access on 04.04.2021]

93. NFPA News. 9 (2005) 1–3.

94. Deliverable 6.1 – Handbook of hydrogen safety: Chapter on LH_2 safety. Pre-normative REsearch for Safe use of Liquid Hydrogen (PRESLHY). https://hysafe.info/wp-content/uploads/sites/3/2021/04/D39_2021-01-PRESLHY_ChapterLH2-v3.pdf [access on 10.05.2021].